THE VERIFICATION OF A DUST-PARTICLE-COUNTER IN CASE OF DIFFERENCES OF PARTICLE SHAPES

Aaron Peix

Bachelor's thesis

September 2012

Degree Programme in
Environmental Engineering

TAMPEREEN AMMATTIKORKEAKOULU

Tampere University of Applied Sciences

ABSTRACT

Tampereen ammattikorkeakoulu
Tampere University of Applied Sciences
Degree Programme in Environmental Engineering

AARON PEIX:
The verification of a dust-particle-counter in case of differences of particle shapes

Bachelor`s thesis 62 pages, appendixes 10 pages
September 2012

The objective of this thesis was to control a dust-particle-counter from the company *Lighthouse*, the *Boulder Counter*. It was to find indications of its ability to distinguish between spherical shaped particles and fibres. For that reason the *Boulder Counter* got compare twice. The first comparison happened with an automatically analysis made by the *DustTrack*. It is a device which monitors the mass concentration. The second comparison is done with a manual made analysis. Therefor was a passive sampling design which gave a direct view to the quantity of extra produced particles.

The tasks relied on the effect known as the *Brownian motion*. Under the right conditions this effect does provide a spatial equilibrium of particles as well as for their concentrations. Additionally all tasks have to be executed perfectly to maintain reproducibility and the accompanied statistical significance.

The results showed enormous discrepancies between the *Boulder Counter* and its comparison opponents. This fact prevented a precise analysis of the *Boulder Counters* ability to distinguish between fibres and spherical particles.

The findings indicated a detection limit for the *Boulder Counter*. It is not able to measure the particles accurately if its detection channels get flooded. This is a common nuisance in the optical detection technology. To conceive the scale of the *Boulder Counters* limitations a further research is recommended before an improved repeat of this task can be granted. Until then is adequate to use the *Boulder Counter* only in environments with as less as possible contamination.

Keywords: Airborne particles, paper dust, particle shapes, fibres, detection

1 CONTENTS

2 INTRODUCTION

Dust in micrometre and even nanometre size range has a not negligible effect on the environment. It affects the health of man and animals through the bronchia and also through ingestion. They can agglomerate with several other hazardous contaminants and as some studies showed can for example cause allergies by agglomeration with elicitors which get inhaled. The inhaled agglomerates enter deep into the bronchia just as any fine dust particle and make the body react on them. Through ingestion can the particles get carried through the food chain while animal breath, eat and get eaten. Any toxic effect can be carried into the next level of the food chain and affects the eater additional to the already present airborne and settled particles. The influences can get accumulated and passed on to the next eater.

In the industry is dust a big problem since airborne particles, especially fine particulates, receives more attention to environmental awareness. In the printing industry is paper the main medium to print on and during the process the paper releases particles and contaminates the air in the factory halls. As a matter of fact the monitoring developed further on. Control devices to monitor the ambiance shaped up in different kinds. For example two kinds of these devices are used in this thesis. One is able to record the mass concentration of dust. The other device counts into the air liberated particles and in addition presents the results sorted in size ranges. The latter is the main part of this thesis. It is the so-called ***B****oulder* ***C****ounter* from the company *Lighthouse* (from now on called **BC**).

The fact that particles show up in different shapes, as spherical particles and as fibres, generates questions to us: Is the BC-device intelligent enough to see the differences between these shapes? How does it look on fibres? - As one big particle or as several smaller particles over the length of the fibre? Beside the two prior mentioned main divisions of airborne particles are there of course individual varieties. Spherical particles exist in all kind of different shapes, just the same as fibres show up in different forms too. The forms of fibres and spheres will be declared later on for this thesis (Chapter 4.2).

All these differences create the previously inquired problematic nature for devices which use optical-detection-technique. Therefore the objective of this thesis is to testify the correct monitoring of the BC in case of paper dust. Which technique the BC exactly uses for the detection, is of course kept confidential by the company Lighthouse. Hence the supervisor Pasi Arvela and i could only estimate that the BC counts and measures the particles by scattering and diffraction of a laser (Chapter 3.2).

The verification has to be made by a comparison of certain results. At first the BC-results are checked against the results of a device to monitor the mass-concentration of airborne particles, the ***D**ust**T**rack* (from now on called **DT**). This device is well proven and trusted to give correct results. Secondly we turn into a passive sampling for a direct view on the particles, especially on the fibres. During this more important sampling the lint is collected and fixed on glass plates. Representative pictures of these lint contaminated plates will be made and analysed by human eye and hand. The effort to compare the PST-results with the BC-results will double because of the 2-dimensional spreading of the fibre magnitude in length and diameter.

The final outcome of the experiment shall provide the quantitative evidence needed for the BCs qualities. This concluding information can lead to different consequences. For instance, if the device turns out as erroneous in case of fibres, the paper processing industry will probably decide against it and demand for more precise equipment. Thence the monitoring appliance industry will have to react and develop or speed up the research for the optical detection techniques to provide the market with a reliable system. Of course, a positive verification of the BC is a welcome situation for every party around the device, the costumers and the developers.

3 EXPERIMENT

3.1 Aim of the experiment

The theoretical idea is to find distinctions or similarities between eventual specific results. Therefor the BC results get compared twice. First with the DT results, which are automatic-results made by a machine (Chapter 4.1). Secondly with the PST results, which is a man-made analysis to control what is actually analysed (Chapter 4.2). Thus we expect quantitative evidence from the experiments. The first and actually easiest theoretical fact has to be proven first, to make sure that the devices operate correct in general. It is about estimating a linear rise of the amount of particles by simply doubling the input of the particle sources. The second and main part of the experiment is less a confirmation of theoretical ideas than more a literally view on the particles, to diversify and measure them manually. Like the comparison of the two different measurable dimensions of the fibres to the BC-results, length and diameter. It shall give us an idea of the prior questioned possibilities of the BC. For example, the cognition that the amount of spherical particles counted in the PST-Test is much less than the number of particles counted by the BC, can lead on to an assumption of repeatedly counted fibres. Otherwise, if the amounts approximately match, the next assumption is that the fibres could show up in the BC-results as the rare 50 to 100µm big particles and as the very rare over 100µm big particles.

All gathered information of these sub-tasks added back together to retrieve the original purpose of this thesis: the verification of the Boulder Counter from the company Lighthouse in the very specific case of the possibility to detect fibres among airborne particles. Parameters and designed operations seem to be promising to fulfil a proper inspection of the BC-device.

3.2 Theoretical background

Particle distribution:

Fine particles do not fall down like any mass with macro dimensions, e.g. a touchable and visible simple stone. With ease they glide with the aerodynamics and thermodynamics through the air and spread out randomly in all three dimensions and change direction constantly. If you observe their performance in a vacuum you would see a straight drop downwards with the drop velocity depending on the site-specific gravitational constant. Because the experiment is done in Tampere, Finland the gravitational constant is there: $g_{Finland} = 9{,}82\ m/s^2$ (Schwartz & Lindau 2002). In a clean-room with standard atmosphere but no polluting airborne particles and no dynamical movement of air, you still observe a movement which does not compare to a steady drop down of a particle as estimated while dropping a stone. The airborne particles still move around and distribute evenly in the down look on the 2D-plane. Additionally they settle slowly, which provides the third dimension, in a down-way direction.

These observations lead to the general known effects of the interaction between gravity and mass. This explains the drop of mass, even very small mass as the probed particle aerosols when its density is bigger than the density of the medium the mass is suspend in. Next to the plunge of mass is an explanation for the sideward spread of the particles necessary. This is supplied by the term of air resistance. The impact of the air resistance is best explained by the Brownian motion and its characteristics.

Brownian motion and Diffusion:

> *Brownian motion* is the irregular wiggling motion of an aerosol particle in still air caused by random variations in the relentless bombardment of gas molecules against the particles. *Diffusion* of aerosol particles is the *net* transport of these particles in a concentration gradient. This transport is always from a region of higher concentration to a region of lower concentration. (Hinds 1999, 150)

The transport of particles is smoothing out the concentration gradients (Mewis & Wagner 2012, 87-88). Equilibrium of particles concentration does not have the effect of none further movement within the aerosol. Considering the *Conversation of Momentum* will there always be motion due to countless impacts between gas molecules and airborne particles. This circumstance can keep the balance of the gradients and can of course also provide fluctuations of these gradients which will arouse more Brownian motion and diffusion. As long as the particles are in their dispersion medium, here air, they will move randomly around and will only stop if they collide with a surface (Hinds 1999, 160).

As per Seinfeld and Pandis (2006, 412) has Brownian motion only a little effect to airborne particles with a 1µm or bigger diameter. A size comparable to the size of a gas molecule like a few nanometres big particle will demonstrate fluctuations in its movement caused by random collisions with the gas molecules. Particles bigger than that experience mostly gravity but Brownian motion is still existent along with the molecules of the medium gas and other airborne particles.

Optical detection:

In line with an internet article of the *Lighthouse* Company, titled “How to Select a Particle Counter for my Cleanroom” (Pole, Lighthouse Worldwide Solutions), is the in the BC applied technology briefly explained at best:

Laser lights or just white light is used as a source within an aerosol stream perfused chamber. When a light ray reaches a particle the ray will get redirected or absorbed. The altered direction or dimmed intensity of the light relates to the size of the particle. These effects allow to measure and count individual particles with photo detection systems. Light scattering or light blocking are the common concepts in the optical detection technology.

In the article is also a hint how the measurement of the particle sizes is conceived. All probed particles become separated in channels due to their sizes. Every channel is represented in microns and particles with the corresponding size get binned and counted in the compatible channel. The BC has 6 channels of the following sizes: 5, 10, 25, 40, 50 and 100 µm (Lighthouse Worldwide Solutions 2012). The hypothesis is: because of the data reliability it is doubtful that the particles between these sizes just get lost and fall out of the analysis. Ergo it is a near expectation that the channel sizes are the upper particle diameter limits for its channels and a bigger than the next smaller channel size particle is not able to enter the smaller channels. This thought actually ends up in the assumption that there is a size range for every channel. How the fabricator of the BC handled the problem of a misdistribution of particles into bigger channels is unknown such as the validity of this hypothesis. On the opposite site it is unclear how the BC shuts down the influx of much smaller than 5µm particles into the first channel or particle bigger than 100µm into the last. Even though a simple sieve could hold back particles bigger than 100µm, where does the estimated size range for the 100µm channel start? The lower and upper limits of the channels still need clarification.

3.3 Design of the experiment

3.3.1 Requirements, Equipment and Application

Stokes-Chamber:

An experiment has to be extricated from the influences of the ambience to be repeatable and to gain representational results. A closed and air-conditioned room is primary necessary. But a room with operators inside has air-movement. This can be crucial for an experiment depending on aerosols which are supposed to settle down without any further distractions. Therefor we use a so called Stokes-Chamber (PICTURE 1). The expression **S**tokes-**C**hamber (from now on called **SC**) derives from its purpose to deflect the inside from aerial oscillations outside during the settlement and keep the conditions of a Stokes´ drag (TABLE 1). In other words it shall keep the air standing still or not faster than just in a very slow, sneaky flow.

PICTURE 1. Stokes Camber (Aaron Peix 2011)

Measurement of the Stokes-Chamber:

Width:	19,5cm
Length:	19,5cm
Height:	60,0cm

Stokes-Chamber mountings:

Within the SC, beneath the bottom are the sampling openings mounted on a board to hold them at a similar level. Its purpose is the combination of the DT and BC. This board is placed between the middle of the two facing sides and the tube openings are mounted in its middle, open side upwards. All mountings and position taken together, the openings are positioned in the middle space below the chamber. The sampling ends of the tubes from BC and DT come from downside into the SC and are attached to the board. These flexible tubes are resistant to electrostatic charging, which can appear by friction between the sucked-in air and particles and the quite narrow interior wall of the tubes.

Passive Sampling Tube (PST):

PICTURE 2. Passive Sampling Tube in Stokes Chamber (Aaron Peix 2011)

PICTURE 3. Sampling Stick for the Passive Sampling Tube (Aaron Peix 2011)

For the passive sampling is a tube designed. This tube is from now on called **PST** which stands for **P**assive **S**ampling **T**ube. The PST is a tube which got an opening in the middle of its length to let matter from above pass through and so can samples just a certain amount at a certain time as demanded. The rest inside is closed and shielded from contaminants, in our case settling airborne particles. It is removable and mounted between two holes about 2cm under the lower edge of the Stokes-Chamber and each of those holes are positioned in the middle of its side and the facing side (PICTURE 2). A quad-

rangular stick by the length of 87cm and a cross section of 1,5cm x 1,5cm (PICTURE 3) is then put sideward into the tube. It provides at one end 5 slots (PICTURE 4) which each carries one microscopy cover slip with each the size of 18mm x 18mm. To catch the settling particles these slips will get exposed to the environment under the opening of the PST with manual made movement of the stick in certain time intervals. To keep the particles grounded on these cover-slips the glass has to be prepared with the Oil-spray "*Dekati DS-515*" within the given instruction by the manufacturer. The oily film is clear and will not tide out of its supposed layer plane and is therefore a fitting substance for our purpose. The intercepted particles glue on the film layer and can only be moved or removed without mechanically actions.

PICTURE 4. Close shot of the 5 slots at the end of the Sampling Stick (Aaron Peix 2011)

Paper, the particle source:

Several aspects point to paper as the chosen particle source. It produces particles as spheres and fibres, and the idea for this thesis came originally out of the paper processing industry. Additionally it provides the base to testify the main theoretical fact for this thesis: the expected linear behaviour of the result-function. The task can be compared with a calibration or control of a spectral analysis based detection device. Contrary to such a calibration for which a standard-solution of a soluble substance gets diluted down in particularly steps, the paper layers will get doubled up during the various processes. In clear words: one lay of the paper produces the standard amount of particles; doubled up to two layers which provide twice that amount; doubled up again to four layers it will provide four times the standard amount.

The chosen particle source is a common copy paper for copier and printers. A 500 sheet parcel of:

Brand:	"*Nordic OFFICE*"
Format:	DIN A4; 21 cm x 29,7 cm
Paper weight:	80 g/m^2
Colour:	white
Article no.:	1049800
NOA:	800693

It is safe to assume that all sheets are identical to each other because of their production which has to assure a negligible variance. To minimize this variance another time we rip always only one paper three times. The results of these paper measurements will be brought together in an average outcome.

The utilisation of the paper:

To produce a settling aerosol with an amount of particles as much as possible it makes sense to rip the paper in the middle down the long side, and for a nearly constant standard emission of particles we use the halves of the ripped paper one upon the other as two layers (doubled up once) and rip them again in their middle of the short side. The out coming quarter-paper-strips get put on top of each other again and ripped in the middle of their short side (doubled up twice). That is the last rip of one sheet of paper because the short (21 cm) and two times halved side of the A4 (format) page is now too narrow to halve it complete and clean another time.

The ripping itself has to be standardized, too. It has to be right above the SC, very close to the top opening to secure that the aerosol settles down into the chamber without distracting drafts but not deep into the chamber to insure to keep height for the areal particle distribution. It is necessary to keep the height of the rupture constant at always the same spot during every ripping process. Hence it makes sense to let the paper hang into the SC and start to rip at the upper short edge of the paper which levels at the top open end of the SC. With a consistently end-to-end performance of throughout 3 seconds the hands are moved symmetrical sideward. This execution leads to the effect that the rupture keeps the height-niveau constantly as demanded. All these performances have to happen the same way in each procedure to provide the required reproducibility.

3.3.2 DustTrack (DT) combined with Boulder Counter (BC)

The first settlement-experiment combines the DT with the BC to check the BCs results by comparing the outcomes over the mass concentration results of the DT (explained detailed in chapter 4.1). The DT was successfully in use before and is therefore well proven. Thus it is predestined to make this general first control. Hence we can see if it would make sense to pursue with the other tasks.

According to lecturer and thesis supervisor Pasi Arvela (2011) the devices have unfortunately different volume flows (Q). The BCs amount of sucked in air during the measurements is intimated by the manufacturer with 27 litres per minute (Q_{BC} = 27 l/min). On the other side is the DTs air consume intimated by its manufacturer with 2,7 litres per minute (Q_{DT} = 2,7 l/min). This difference creates a problem: Because the Q_{BC} is 10 times bigger than the Q_{DT} (3-2) but both devices use the same kind of tubes with the same diameter, the velocity of the into the BCs streaming air is 10 times quicker than the DCs. It has to be balanced to eliminate an uneven distribution of the particles between these

devices. The numerous-similarity is a welcome incident. It helps to find an easy solution: open up the sampling tube opening of the BC by the same factor it demands more air during the sampling, the factor 10, will slow the airflow down by the same factor. This fact is described mathematically by the *Continuity Equation* (3-5) and can be comprehended in the following calculation.

We want the volume flow rate of the BC and the DT to be equal:

$$Q_{DT} \neq Q_{BC} \tag{3-1}$$

$$10\,Q_{DT} = Q_{BC} \quad \| : 10 \tag{3-2}$$

$$\Rightarrow \quad Q_{DT} = \frac{Q_{BC}}{10} \quad \| Q = A * v \tag{3-3}$$

$$\Rightarrow \quad \underline{Q_{DT} = A_{BC} * \frac{v_{BC}}{10}} \quad . \tag{3-4}$$

The result implements: the velocity of the income aerosol has to be slowed down by the factor 10. Therefor we use an applied version of the *Continuity Equation* (3-5), which should show us how the problem will be solved:

$$\boxed{\rho_1 * Q_1 = \rho_2 * Q_2} \quad , \tag{3-5}$$

with ρ as the density of air and as it is the same air as fluid at state 1 and state 2, described in (3-6), is the problem solved as followed:

$$\rho_1 = \rho_2 \tag{3-6}$$

$$\Rightarrow \rho_1 * Q_1 = \rho_1 * Q_2 \quad | : \rho_1 \tag{3-7}$$

$$\Rightarrow \quad Q_1 = Q_2 \quad \| \, Q = A * v \tag{3-8}$$

$$\Rightarrow A_1 * v_1 = A_2 * v_2 \quad \left\| \; v_2 = \frac{v_1}{10} \right. \tag{3-9}$$

$$\Rightarrow A_1 * v_1 = A_2 * \frac{v_1}{10} \quad | * 10 \tag{3-10}$$

$$\Rightarrow 10A_1 * v_1 = A_2 * v_1 \quad | : v_1 \tag{3-11}$$

$$\Rightarrow \quad \underline{10\,A_1 = A_2} \quad . \tag{3-12}$$

As predicted before the result proves that the sampling end has to be opened up by the factor 10 to equilibrate the velocities of the incoming aerosols (3-12).

The BC and the DT have to be programmed before declaring the sampling time and the time-constant which set the interval of measurements during the recording time. The recording time for every rip is set to 2 minutes for both devices and both measure every second. This reveals 120 measurements during the sampling for every paper-rip. After the sampling start it takes 4 seconds until the eventually ripping of the paper starts. This is the amount of time which flies while standing up from the floor where the devices are placed and getting the paper in position for the particle production process. These 4 seconds plus the 3 seconds for the ripping-action accumulate to a 7 seconds time delay until the complete particle production is done and the full number of particles is set free, distributed in the upper chamber area and settling. Just then we can estimate a representative result from the devices.

Furthermore is there a settling time to consider before the devices recognize the first particles, to compare it with the reality. Based on the fact that gravity interacts stronger with heavier particles and that the BCs limitation in size ranges until 100µm, it occurs that particles about 100µm big and a density of 1000 g/cm^3 (Hinds 1999, 10) will be the first to reach the SC ground and to vanish into the sampling-tubes-openings. A particle of 100µm is therefor used to calculate the theoretical settling-time.

The sedimentation velocity w_f (Stieß 2005) is calculated through:

$$\boxed{{w_f}^2 = \frac{4}{3} * \frac{\rho_p - \rho_f}{\rho_f} * \frac{g * d_p}{c_w(Re_d)}} \quad , \qquad (3\text{-}13)$$

with d_p diameter of particle

g gravity constant, in Finland : $g_{Finland} = 9{,}82\ \frac{m}{s^2}$

ρ_p density of particles, $\rho_p = 1000\ \frac{kg}{m^3}$

ρ_f density of the fluid, Air : $\rho_{air} = 1{,}20\ \frac{kg}{m^3}$

$c_w(Re_d)$ drag coefficient depending on the Reynolds number Re_d.

The drag coefficient $c_w(Re_d)$ depends on the Reynolds number Re_d and varies with it:

TABLE 1. Division drags referring to the Reynolds number

Stokes drag	$Re_d < 0{,}25$	$c_w(Re_d) = \frac{24}{Re_d}$
Transition drag	$0{,}25 < Re_d < 10^3$	$c_w(Re_d) = \frac{1}{3} * \left[\sqrt{\frac{72}{Re} + 1}\right]$
Newton drag	$10^3 < Re_d < 2 * 10^5$	$c_w(Re_d) \approx 0{,}44$

Therefor has the Reynolds number Re_d to be calculated previously:

$$Re_d = \frac{\bar{v} * d}{\nu} \quad , \qquad (3\text{-}14)$$

with $\bar{v}$ average velocity of the drag

d diameter of the Stokes-Chamber

ν kinematic viscosity of the medium.

All the three parameter in the Reynolds number formulary have to be worked out first. The kinematic viscosity is calculated out of the quotient of the dynamic viscosity η_{air} (3-22) and the air density ρ_{Air} (3-20). The air density and viscosities are constituted to the conditions of the **N**ormal **T**emperature and **P**ressure (**NTP**) at 20°C or 293,15 K and 1 atm or 1,013 bar (The Engineering ToolBox) which are the closest to the conditions during the experiments. The values are given in tables out of professional literature or can also be calculated (APPENDIX 1). The results out of (3-25), (3-30) and (3-34), which are noticed in the APPENDIX 1, get set into (3-14) to calculate the Reynolds number:

$$Re_d = \frac{0{,}013\ \cancel{m} * 0{,}195\ \frac{\cancel{m}\ s}{s\ \cancel{m}^2}}{1{,}51 * 10^{-5}} \qquad (3\text{-}35)$$

$$\underline{Re_d = 168{,}11} \quad . \qquad (3\text{-}36)$$

This Reynolds number value (3-36) indicates that the drag actually outreaches the estimated Stokes´ drag behaviour (Table 1) within the SC. The air draft created by the suction of the devices oppose against the principle of the Stokes´ drag. The combined volume flows move the air within the Stokes-Chamber during the sampling too intense to warrant a not more than a creeping air current. This effect actually deranges the premises for an undisturbed distribution of particles inside the aerosol and its settlement. After discussion with the thesis supervisor Pasi Arvela the agreement came up to cherish with a combination of BC and DT for this test series for a better comparability.

The drag coefficient c_w can now be calculated with the Reynolds number result. The associated formulary depends on the value of the Reynolds number (3-36), has to be chosen out of the 3 possibilities (Table 1) and applied (3-37):

$$c_w(Re_d) = \frac{1}{3} * \left[\sqrt{\frac{72}{Re} + 1}\right]^2 \quad , \tag{3-37}$$

$$c_w(Re_d) = \frac{1}{3} * \left[\sqrt{\frac{72}{168{,}11} + 1}\right]^2 \tag{3-38}$$

$$\underline{c_w(Re_d) = 0{,}912} \quad . \tag{3-39}$$

As prior explained for the settlement velocity (3-13) is a particle diameter d_p of 100µm chosen because it is the heaviest particle to monitor and will be the first to reach the SCs bottom. All elements for the settlement velocity w_f are now determined and inclinable:

$$w_{f,100\mu m}^2 = \frac{4}{3} * \frac{\rho_p - \rho_f}{\rho_f} * \frac{g * d_p}{c_w(Re_d)} \quad , \tag{3-40}$$

$$w_{f,100\mu m}^2 = \frac{4}{3} * \frac{(1000 - 1{,}20)\ \cancel{kg}\ \cancel{m^3}}{1{,}20\ \cancel{kg}\ \cancel{m^3}} * \frac{9{,}82\ m * 100 * 10^{-6}\ m}{s^2 \quad 0{,}913} \tag{3-41}$$

$$w_{f,100\mu m}^2 = \frac{4}{3} * 832{,}33 * 1{,}076 * 10^{-3} \frac{m^2}{s^2} \quad (3\text{-}42)$$

$$w_{f,100\mu m}^2 = 1{,}194 \frac{m^2}{s^2} \quad (3\text{-}43)$$

$$w_{f,100\mu m} = \sqrt{w_{f,100\mu m}^2} = \sqrt{1{,}194 \frac{m^2}{s^2}} \quad (3\text{-}44)$$

$$\underline{\underline{w_{f,100\mu m} = 1{,}093 \frac{m}{s}}} = \underline{\underline{109{,}291 \frac{cm}{s}}} \quad . \quad (3\text{-}45)$$

The outcome (3-45) explains that a particle with the diameter of 100µm is estimated to fall with a rate of 109,3cm per second or 1,093m per second. With the knowledge of the fall metrics and the fall rate it is possible to calculate a theoretical settlement time t_{settle}. The height of the SC h_{SC} is 60,0cm and is assumed as the distance the sphere-particle has to travel.

$$t_{settle} = \frac{h_{SC}}{w_f} \quad \left\| w_{f,100\mu m} = 1{,}093 \frac{m}{s} \right. \quad , \quad (3\text{-}46)$$

$$t_{settle,100\mu m} = \frac{0{,}6 \cancel{m} \; s}{1{,}093 \cancel{m}} \quad (3\text{-}47)$$

$$\underline{t_{settle,100\mu m} = 0{,}549 \; s} \quad . \quad (3\text{-}48)$$

This calculated values (3-45) and (3-48) appear quite absurd. A 100µm-particle is unlikely to drop with this high velocity. Hence this circumstance claims reconsideration or just a recalculation with another formulary from a subject book from Hinds (1999) proposed by the thesis supervisor (Arvela 2011). The revaluation is found in Appendix 2. Here are the results which can be compared directly to (3-45) and (3-48):

$$\underline{\underline{v_{TS,100\mu m} = 1{,}12\ \frac{m}{s} = 112{,}2\ \frac{cm}{s}}} \quad (3\text{-}58)$$

$$\underline{\underline{t_{settle,100\mu m} = 0{,}53\ s}} \quad (3\text{-}61)$$

The new settlement speed of a 100µm is 1,12m per second (3-58) and compares quite similar to the first outcome (3-45) with 1,09m per second. The result figures and tables (Chapter 4) of the devices will show if these theoretical ascertained settling times will prevail. Yet are both results reasonably implausible and are unlikely to get confirmed by any empirical purchased data. These theoretical settling times depend only on the drop of the particle, in which its way will not be disturbed by Brownian motion, electric fields, drags or any other influences, nevertheless the different internal properties of aerosols.

The aerosol property which concerns the most in this case is the movement behaviour in a drag. Air can pass through an aerosol or pass around it. The air will go the path of less resistance (Hinds 1999, 380). This depends on the particle concentration of the cloud. “At a low particle concentration, the air will pass through the cloud, and each particle will experience” (Hinds 1999, 380) the settlement velocity. “At a sufficiently high particle concentration, the resistance to airflow through the cloud will be so great that the air will flow around the cloud,” (Hinds 1999, 380). In this case the air is flowing around the cloud and the velocity of the particles inside the cloud is zero. These are extremes and intermediary circumstances operate between these mechanisms (Hinds 1999, 380).

The similarity of (3-13) and (3-49) does not surprise. The two formulas are despite one factor actually just in their image different. While in (3-49) every quantity got written into one complex fractional term, are in (3-13) all factors accordingly to their influences separated into single factor terms within the whole formula. Other formulas to determinate the settling velocity were applied, but none delivered conciliate results. For that reason and because sources

feature derivations to the equation (www.mvsengineering.com 2012), became only the two previously formulas (3-13) and (3-49) utilized. (3-13) is the preferred formula. It is complete and not simplified, instead of (3-49) in which the density differences, coming out of the contrary forces of gravity and air resistance, got left out.

The sampling results are saved on the intern hard drives of the devices. The BC memorizes up to a maximum of 3000 data. Taken an every second measurement throughout 120 seconds for every test and every paper used three times as 1, 2 and 4 layers the BC is able to record the data of 8 papers. Ensuing to the recording the data get copied over to a computer, converted and are then ready for further adaptations. The information gained by the experiment has to be elaborated. Differences between the by the devices putted out units of the current results will be solved mathematically (Chapter 4.1) to make them comparable.

As everywhere in nature is a certain amount of particles already in the air. This background should be eliminated from the outcomes to analyse. Hence only the extra produced airborne particles are set to be use in the results. Therefor is an extra sampling necessary. In consideration of this issue and correspondence with the thesis supervisor Pasi Arvela (2011) a 6 minute run of the BC and the DT without any artificial particles feed got scheduled. This will give enough data to generate an adequate average background value which will be deducted from further edited results.

3.3.3 Passive sampling tube (PST)

Secondly in time, but as the primary and most important experiment, comes the PST-test (PST is explained detailed in chapter 3.3.1). The objective is to gain representative still images of the particle areal distribution at a specific moment in the same height the BC-/DT-sampling openings were before, to maintain comparable results. The freeze images will be examined for particles and fibres which get measured, recorded and presented to compare the outcomes of the two experiments.

The idea is quite simple. The PST is set at the position for sampling likewise the BC and DT devices before. The particles must be provided exactly the same as before with the BC and DT (Chapter 3.3.1) by ripping paper and have to get the same down-way to spread in the air similar and evenly to warrant that every still will be representative equal at any spot of the plane at the height of the sampling, direct below the Stokes-Chamber. The findings of the PST analysis are pure quantity and can then be compared directly with quantity of the BC particle counts.

The sampling process is done manual and therefore it demands a bigger time consume. It is a disadvantage for the precision of the passive sampling that our equipment limits us to 5 stills over a single sampling procedure and therefor has 5 moments to be found which represent 5 featuring key points in the BC-/DT-results. This specific moments will carve out of the characteristically attributes of the tables of the DT-sampling (FIGURE 13) in results chapter 4.1.

The to-secure-the-particle-image prepared glass slips get set in position inside the PST by the positioning rod (Images 4 and 5). They are not allowed to get contaminated by the background impurity of the air. Hence it is during the preparation and also during the sampling necessary to keep the glass slips covered.

The interval in which the glass-slip-slots will be skipped through is chosen to:

TABLE 2. Time interval for the PST sampling

Slot	Sampling Clock in Seconds	Seconds to sample and to skip Slot afterwards
1	0 – 20	20
2	20 – 40	20
3	40 – 60	20
4	60 – 80	20
5	80 - 120	40

Recognize that the time-interval sums up to 2 minutes which is the same amount the BC and the DT uses. The 20-Seconds-Intervall accrues in the DT results (Figure 4). It shows that approximately every 20 second appears a significant change of the slopes in the graph function. Although the last slop change alters to a slow steady decrease during 40 seconds. This effect comes toward our equipment limitation of only 5 slots and thus ensures representative and comparable results within the possibility of 5 graphic key points.

The constraint of comparability forces the procedures to be equal. Like in the BC-/DT- experiment the particle production produces next to particles also a temporally delay which has to be inducted into the PST procedure, too. Starting with the positioning of the first slot it has to consume 4 seconds to get the paper in position and then 3 seconds to actually rip it through the long side. A stop watch on a computer screen gave signal when to slide the rod through the PST from slot to slot until the 120 seconds have passed. Then the particle loaded glass slips have to get as quick as possible in custody to preserve them from further contamination.

Custody of samples:

After a sampling line is done as explained previously and the all five glass slips in the slots are loaded with the from paper released particles, the slips have to get tinned promptly to avoid ulterior contamination by background contaminants. Therefor are Petri dishes envisaged and prepared. On the dish cover is written: The number of the paper, the layer count and the status of the sample. The possible problem slots in brackets or just a hook for a problem free sampling and if it is from the single paper line or from the double paper line (PICTURE 5).

PICTURE 5. Labelling of custody dishes (Aaron Peix 2011)

To distinguish the glass slips from each other, they get tagged with a marker before the oil-spray preparation. The upper right corner of each of them gets marked with a number of dots equal to address number of the associated slots (PICTURE 6). One prevents any other confusion with the mark location by keeping the loaded side upside in the Petri dish in addition to the distinction related to the associated papers written on the dishes themselves.

PICTURE 6. Numerous labelling of 5 glass slips for the sampling slots of the sampling stick (Aaron Peix 2011)

4 RESULTS

An average value for the BC and the DT is computed out of 5 series of tests. This has to be done to generate a statistical significance of the results. Furthermore include all measurements next to the produced particles the background contamination of the room air as well. The BC and DT tools do actually imbibe all particles inside of the SC. Even those which are too small and too light to sediment contrary to the *Brownian motion* and those measurable particles which move untypically toward the flux from outside of the SC. That is why an encompassing background sampling had to be made. This takes no effect to the PST-Task because this sampling depends solo on the sedimentation of the released particles. For the BC and the DT an average gets calculated out of the Background data for both machines. It gets immediately subtracted from the associated out coming data and will not be mentioned anymore. For a closer examination these data are exhibited in Appendix 3.

4.1 DustTrack (DT) combined with the Boulder Counter (BC)

The BC results get averaged and for a better comparability normalised into a concentration rendition like the results of the DT are displayed too. Out of this normalisation appear no integer numbers. Because the BC recognizes particles only as a whole and a count of particles is also only done without fragments, is every outcome rounded up to its next full number (TABLE 2). Furthermore are the particle concentrations in counts per litre and counts per cubic meter (TABLE 2).

TABLE 3. BC results, average particle concentrations for 1, 2 and 4 layers

Averages **1 Layer**		**Concentrations :**		
		c(N) in 1/ Liter	→ up rounded result	c(N) in 1/ cubicmeter
particle Sizes	5µm :	877,29	878	878000
	10µm :	78,88	79	79000
	25µm :	2,05	3	3000
	40µm :	0,23	1	1000
	50µm :	0,07	1	1000
	100µm :	0,00	0	0
Averages **2 Layer**		**Concentrations :**		
		c(N) in 1/ Liter	→ up rounded result	c(N) in 1/ cubicmeter
particle Sizes	5µm :	1352,90	1353	1353000
	10µm :	107,85	108	108000
	25µm :	2,24	3	3000
	40µm :	0,25	1	1000
	50µm :	0,09	1	1000
	100µm :	0,00	0	0
Averages **4 Layer**		**Concentrations :**		
		c(N) in 1/ Liter	→ up rounded result	c(N) in 1/ cubicmeter
particle Sizes	5µm :	2166,82	2167	2167000
	10µm :	174,61	175	175000
	25µm :	4,47	5	5000
	40µm :	0,44	1	1000
	50µm :	0,67	1	1000
	100µm :	0,00	0	0

TABLE 4. BC results, standard deviations

standard deviation	5µm	10µm	25µm	40µm	50µm	100µm	all sizes
1 Layer	376,79	42,85	1,89	0,31	0,18	0,00	216,68
2 Layer	651,39	61,31	2,08	0,32	0,20	0,00	355,04
4 Layer	1014,79	96,52	3,74	0,41	0,91	0,00	559,93
all layers	769,67	72,81	2,74	0,35	0,56	0,00	405,05

The size associated values get summed up for every layer to verify the performance of the BC in the first place (TABLE 5). The general function of the BC instrument could be approved by a linear rise of the particle growth along with the growth of the particle source output. To proof and to present the general propriety comprises FIGURE 1 the summed particle of every size over the paper layers as particle sources.

TABLE 5. BC results, summed particles for 1, 2 and 4 layers per litre

∑ c(N) of all sizes	Layers
962	1
1466	2
2349	4

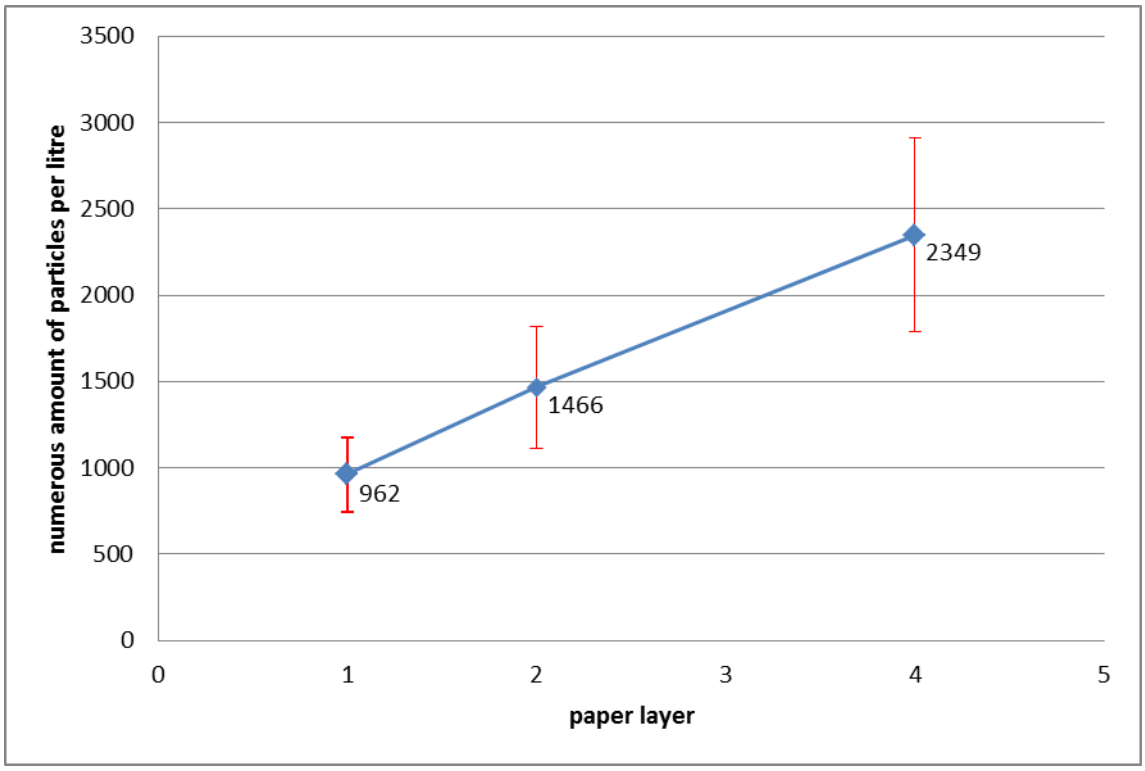

FIGURE 1. BC results, average particle concentration over paper layers with standard deviations for every layer

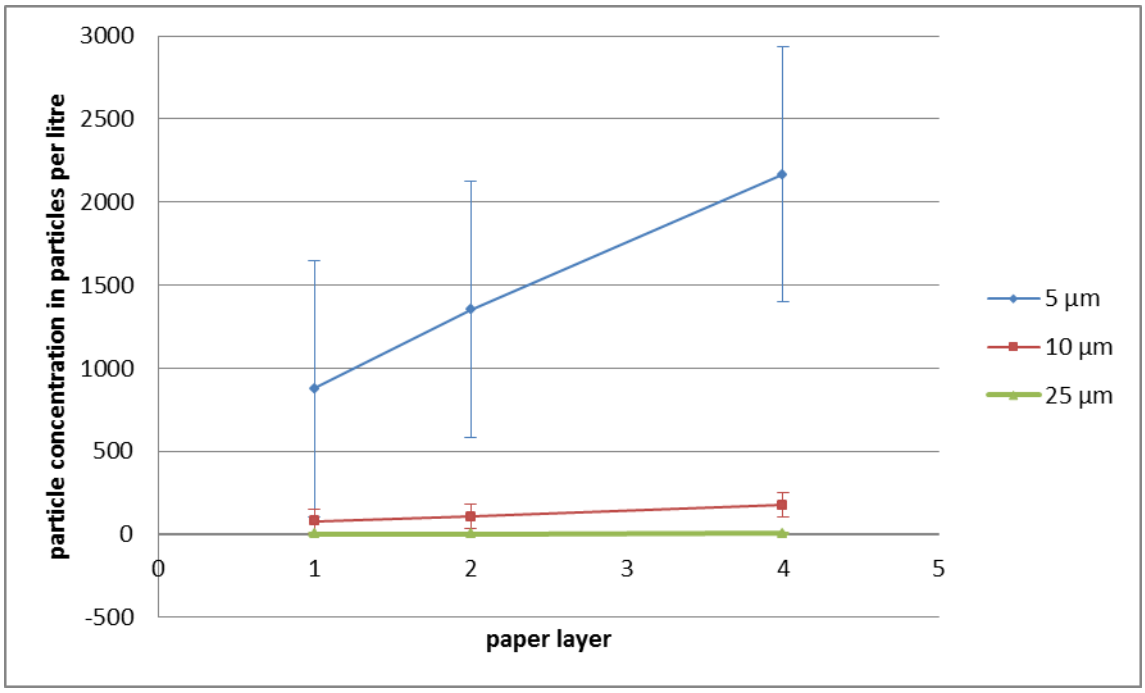

FIGURE 2. BC results, average amount of particles for 5, 10 and 25 µm over paper layer (linear scale)

Moreover enables TABLE 3 a graph to illustrate the behaviour of the single size ranges over the increasing paper layers. Because of the big discrepancy between the particle concentrations $c(N)$ of their size ranges, the three biggest (FIGURE 3) diameter ranges get separated from the three smallest (FIGURE 2) to facilitate an investigable figure. They get shown in a linear scale because a logarithmic scale will hinder the illustration of the 100µm series and its standard deviation (TABLE 4).

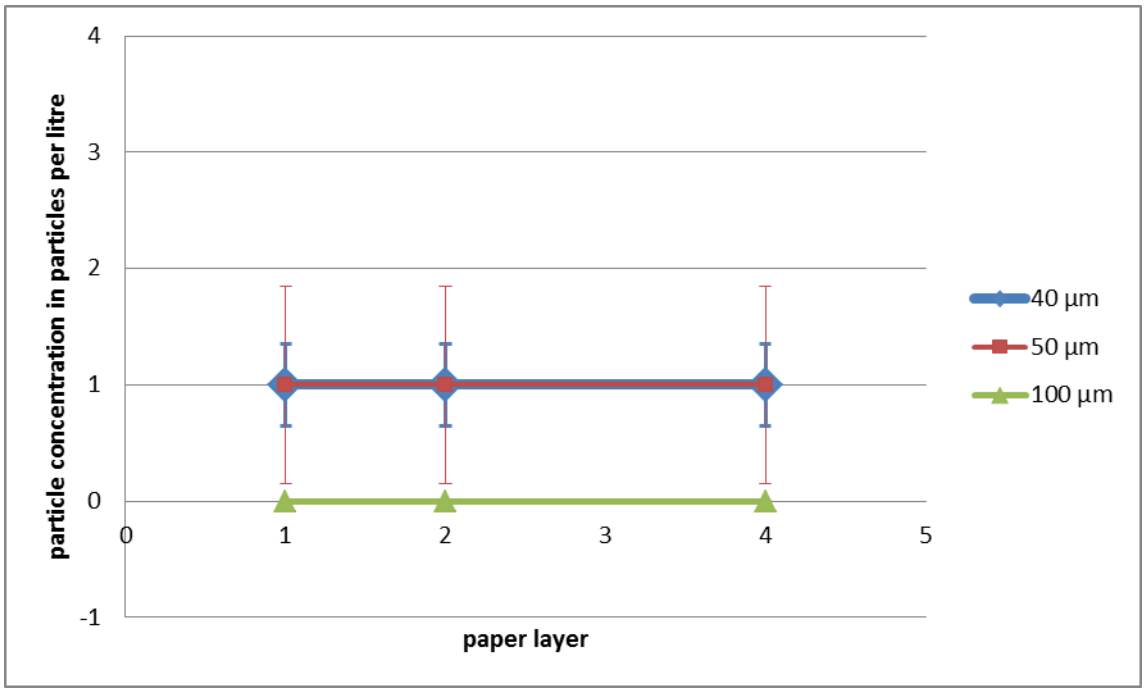

FIGURE 3. BC results, average amount of particles for 40, 50 and 100 µm over paper layer (linear scale)

The DT implement is recommended (Arvela 2011) to control the BCs measurement as the first step of the verification. Both devices run simultaneously during the samplings. FIGURE 4 shows the average mass concentration caused by the release particles from 1 layer, 2 layers and 4 layers of paper in the SC during the sampling time. The unit for the mass concentration $c(m)$ issued by the DT is given in $\frac{mg}{m^3}$ which is equal to $\frac{\mu g}{l}$.

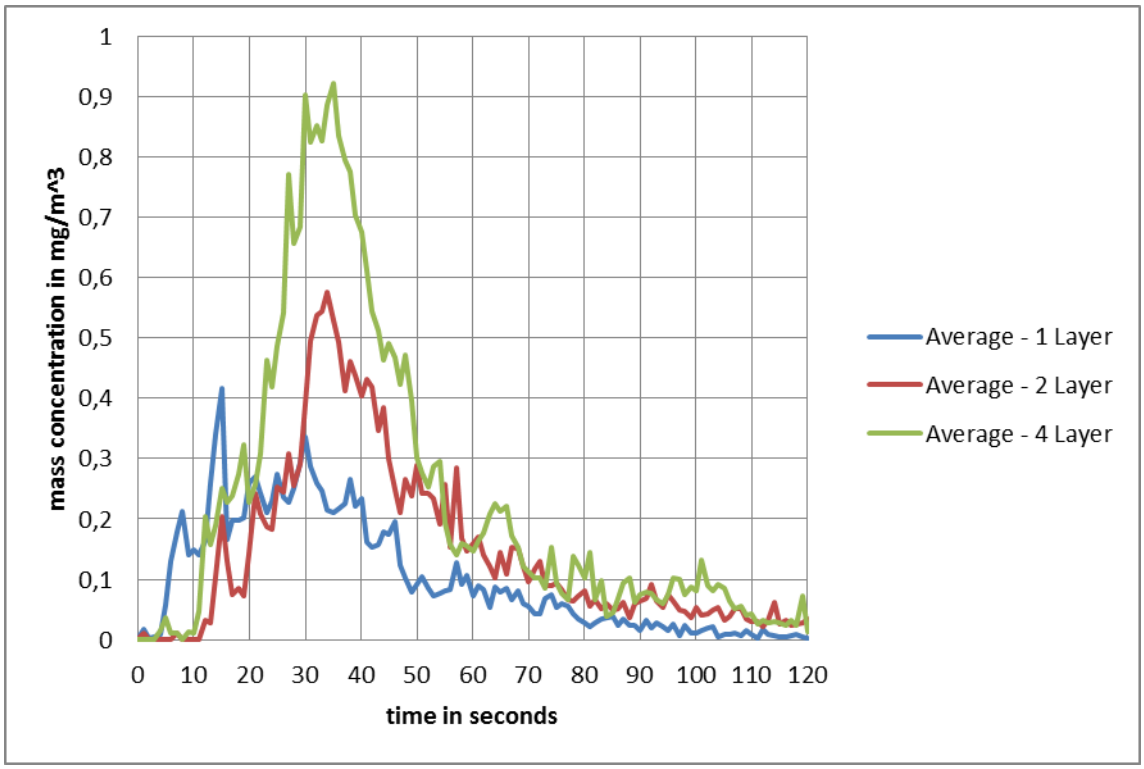

FIGURE 4. DT results, Average mass concentration over sampling time

The DT can neither recognise single particles nor distinguish between the different sizes and shapes of the particles. Hence is an optimally comparison done by comparing the mass concentration $c(m)$ released by the paper layers. The BC results have to be converted into mass m and mass concentration $c(m)$. In Appendix 4 a table is placed in which this process is step by step traceable. To start the table procedure it is a must to ordain the volume of a particle first. It has to be assigned specifically to the sizes of the BC channels. In other words: the volumes (4-1) of the particles with a detectable diameter have to be calculated.

$$V_{p,i} = \frac{4}{3} * \pi * \left(\frac{d_i}{2}\right)^3 \quad , \qquad (4\text{-}1)$$

with $V_{p,i}$ Volume of a specific particle

d_i Diameter of the specific particle .

The formula for a volume of a sphere (4-1) has to be completed with the needed diameter of the particle.

The results in Appendix 4 start with the volumes of the by the BC detectable and recognizable particles assigned to their diameter and ends with the $c(m)$ of every size range and segmented into paper layers (red marked in Appendix 4). Notwithstanding is further analysis only achievable with a comparison of the cumulated mass concentration. Therefor is the cumulative mass (blue marked in Appendix 4) divided by the sucked in air volume during the measurement $V_{measure}$. The outcomes for every layer are shown in TABLE 6. The DT gives out its results already in mass concentrations which are analogous with the calculated concentrations (Appendix 4) after they got summed up (TABLE 7). Both tables can now be compared directly.

TABLE 7. BC results, into c(m) converted cumulative counts

cumulative c(m) in µg/litre	
1 Layer	0,1277
2 Layer	0,1773
3 Layer	0,3283

TABLE 6. DT results, cumulative mass concentration

cumulative c(m) in µg/litre	
1 Layer	12,427
2 Layer	17,661
3 Layer	28,015

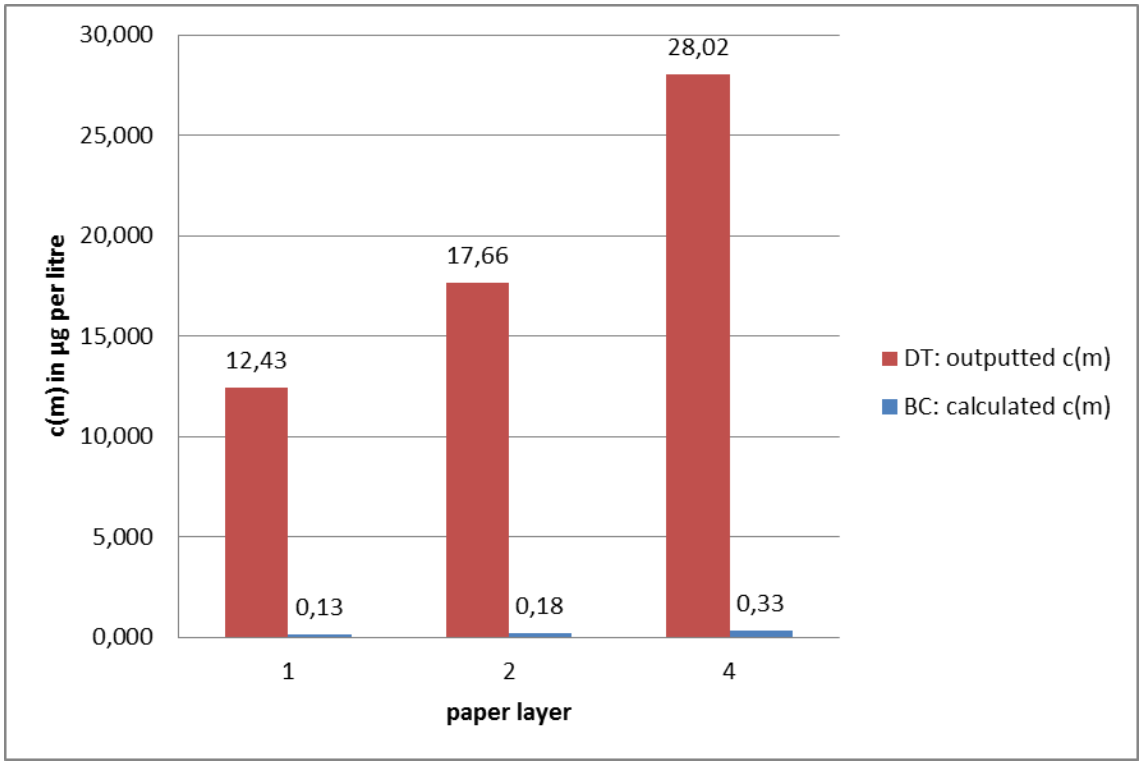

Figure 5. Bar chart comparison of the mass concentration out coming from the BC and the DT

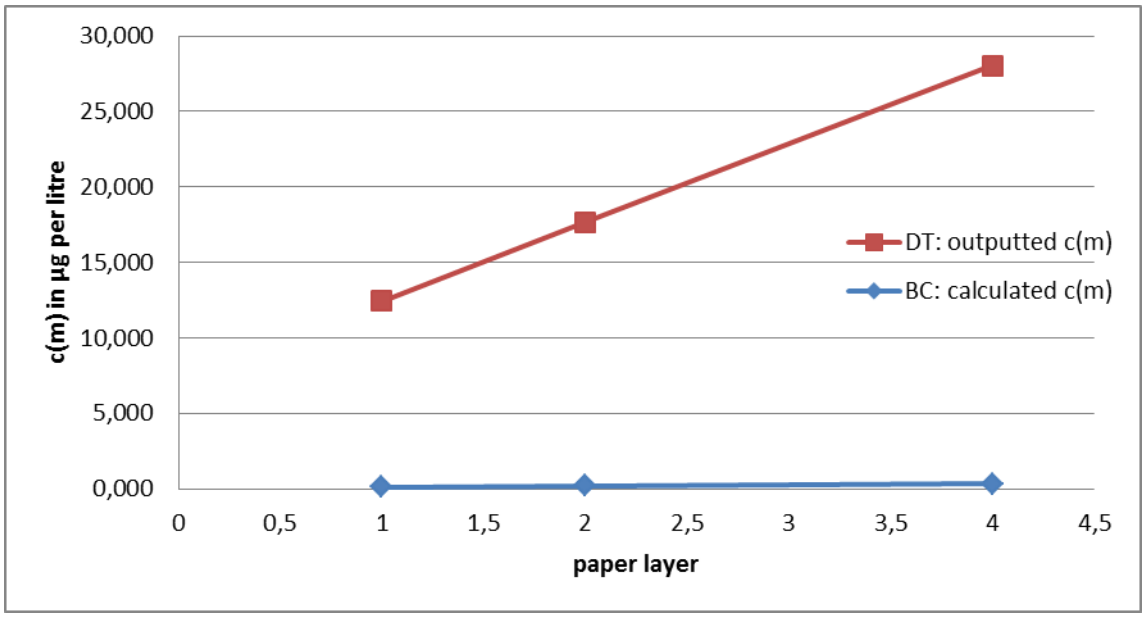

FIGURE 6. Linear comparison of the mass concentration out coming from the BC and the DT

The results out of TABLE 6 and 7 do totally vary from each other, best shown in FIGURE 5 and 6. Whereby FIGURE 5 presents the results in a bar-chart for a better visualisation and in FIGURE 6 it is displayed in the usual linear comparison. To find any similarities between the device-findings are more graphs prepared. In FIGURE 7 and 8 are the DT and BC results exhibited particular to make it possible to observe their behaviour separately.

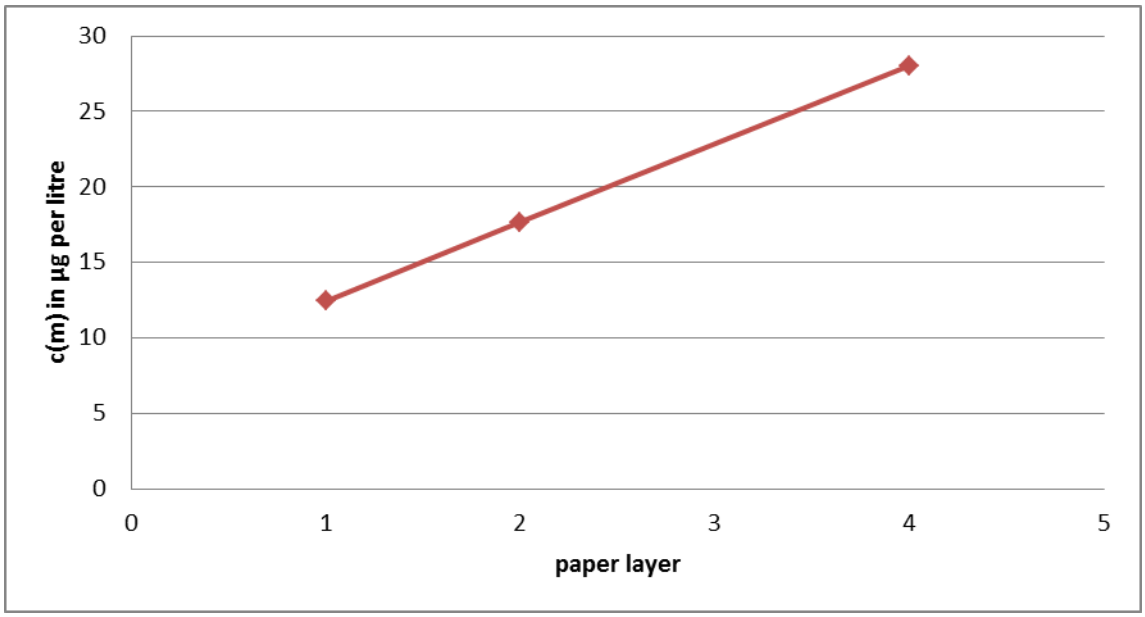

FIGURE 7. DT results, cumulative mass concentration of layers over paper layer

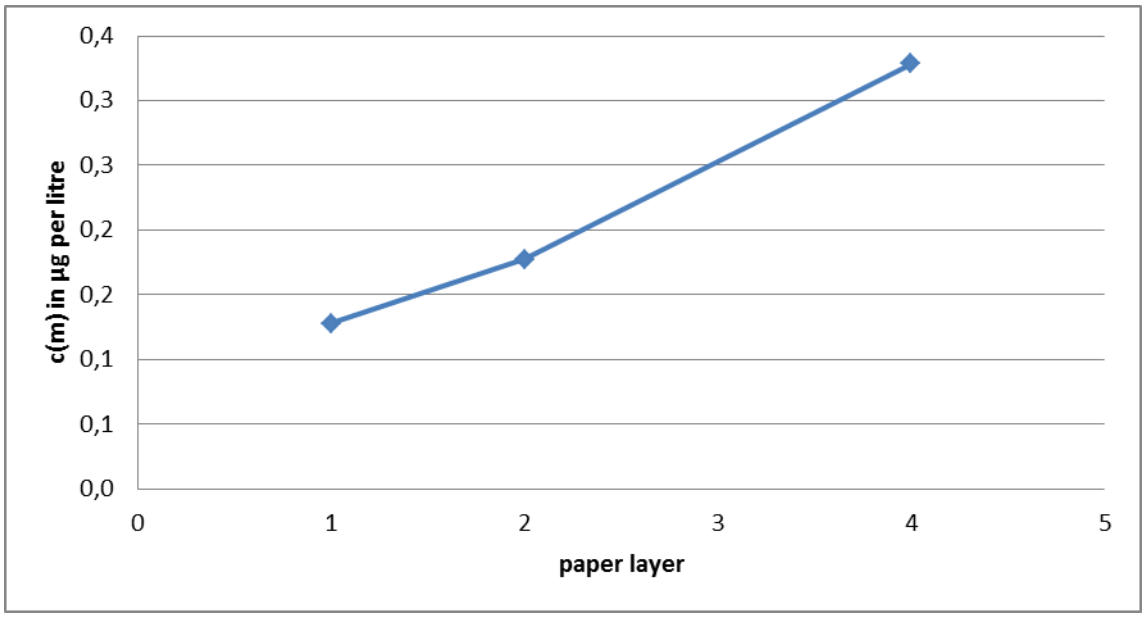

FIGURE 8. BC results, cumulative mass concentration of layers over paper layer

The primary information of Appendix 4 is more a step for the comparison of the apparatuses. Nevertheless, they do exemplify the manner of the particles within the detectable size ranges. A relative graph issues this comportment in FIGURE 9.

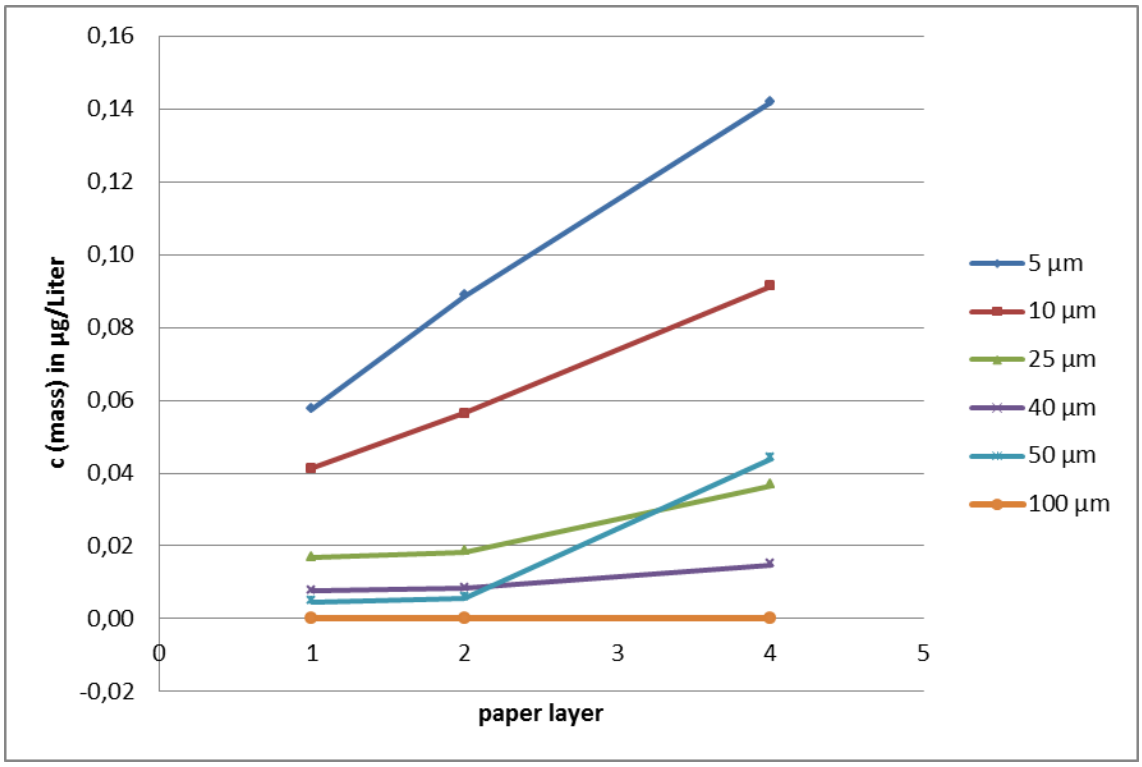

FIGURE 9. BC results, calculated average mass concentration of a 2 minutes sampling

Because of the big differences between BC and DT results in FIGURE 7 and 8 is a closer look recommendable. For that reason are three more illustrations made. These expose the mass concentrations of every second during the measurement of the BC and DT for the layers in particular and compare them to each other (FIGURE 10, 11, 12). The BCs mass concentration is accumulated out of the single size ranges and the maxima peaks are labelled. The related tables are found in Appendix 5.

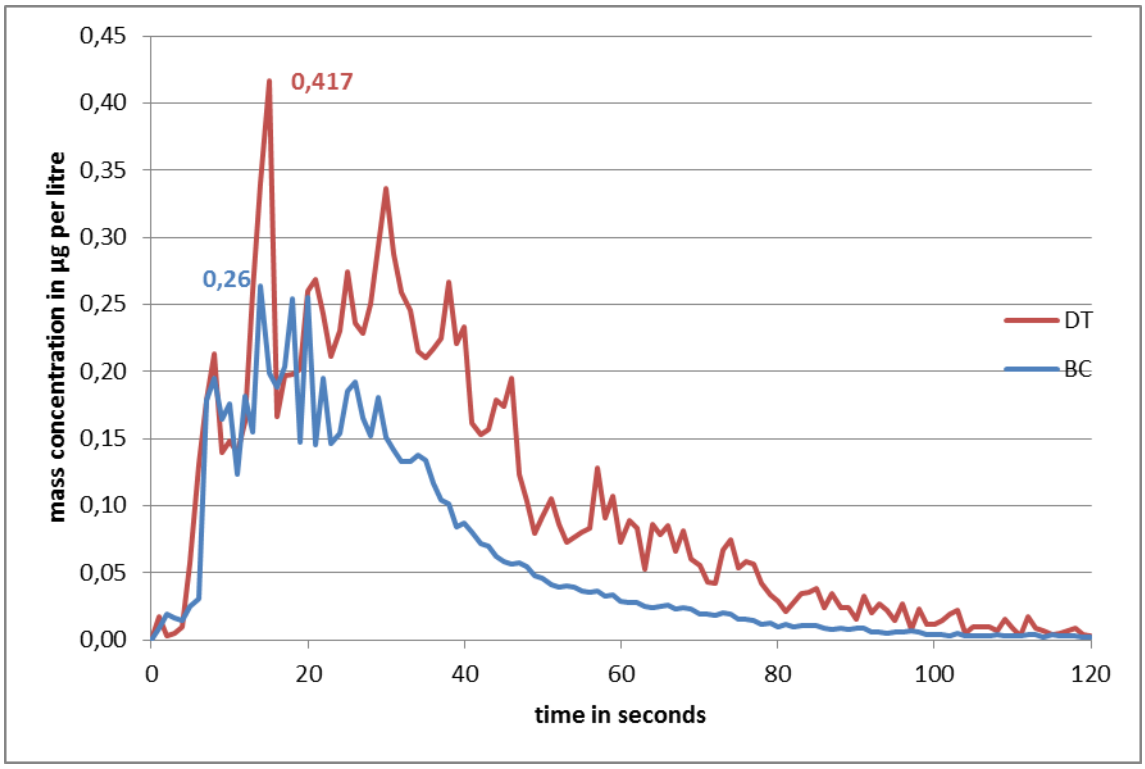

FIGURE 10. BC and DT comparison, 1 layer results in µg per litre over seconds

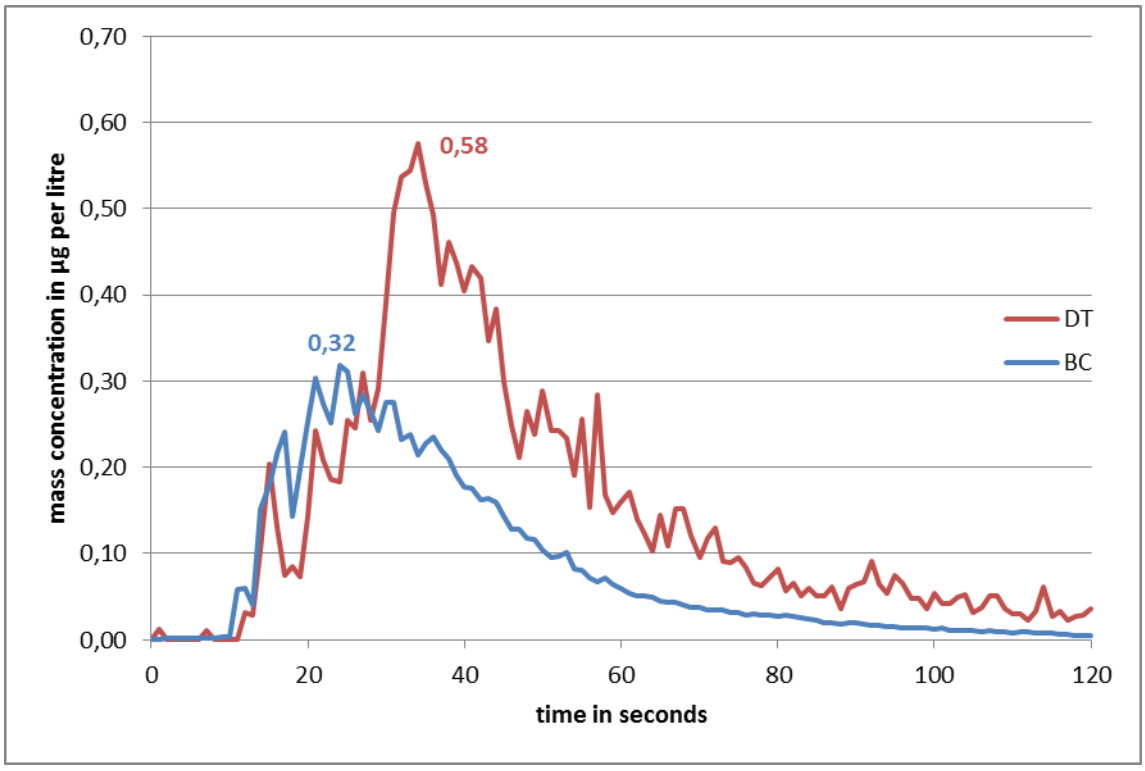

FIGURE 11. BC and DT comparison, 2 layer results in µg per litre over seconds

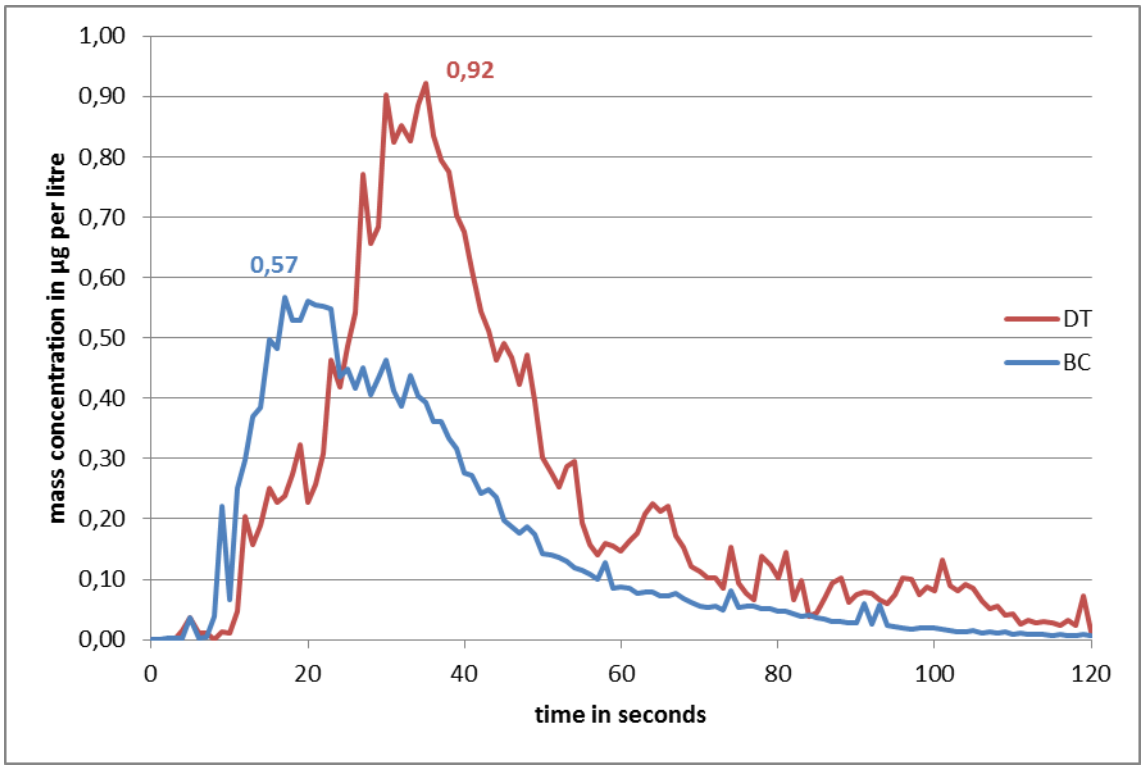

FIGURE 12. BC and DT comparison, 4 layer results in µg per litre over seconds

4.2 Passive sampling

4.2.1 Procedure and analysis

The very best way to verify the BC would be by control all sampling results in the time interval the BC was adjusted to, but the effort of time and manual labour would be invaluable. The PST analysis is done man-made and will be explained hereinafter. To minimize the amount of work within an acceptable amount of data the results get by the reliable tool, the *DustTrack* (DT), inspected for common behaviour. Out of FIGURE 4 emerge some characteristics in a 20 second time period. They got illustrated and delineated in FIGURE 13.

As explained prior in chapter 3.3.1 under “Passive Sampling Tune (PST)” the PST-Stick can hosts 5 slots which give us the opportunity to cut the “every second through 2 minutes” sampling down into a “five samplings through 2 minutes” measurement series. The worked out five steps for the new PST sampling interval is depicted in FIGURE 13.

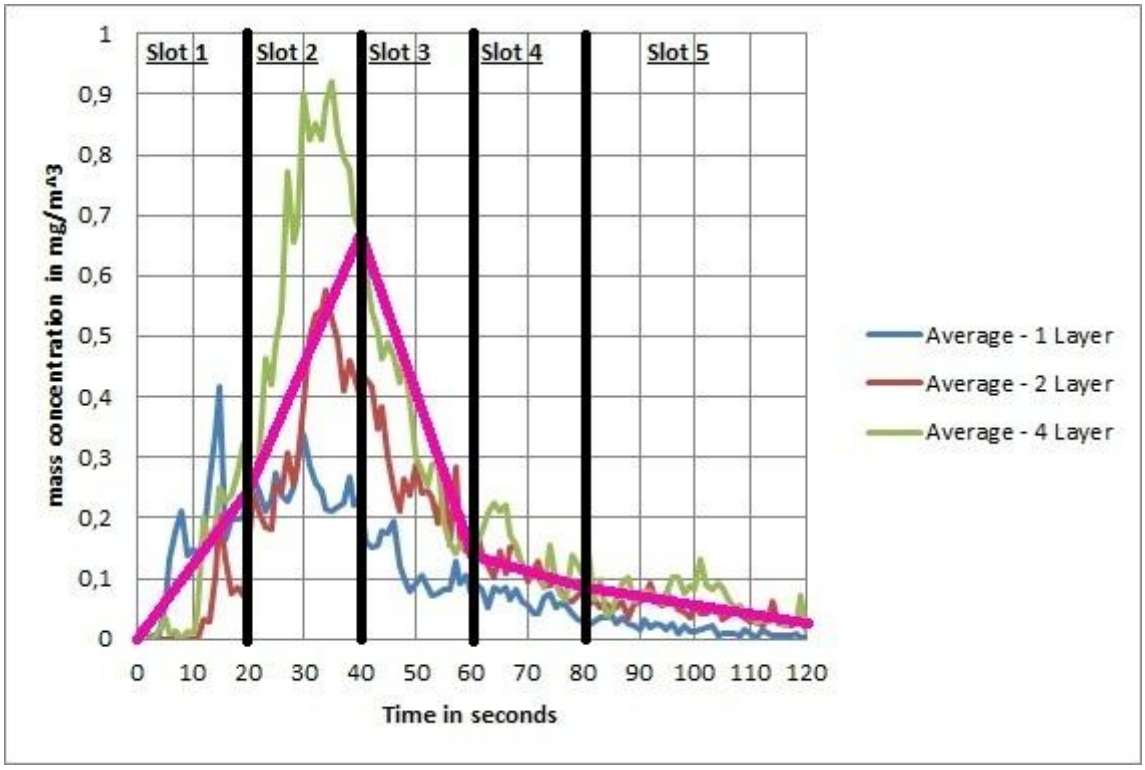

FIGURE 13. Illustration of the time segmentation for the PST Slots out of DT results (FIGURE 4)

For Slot 1 and 2 carve out significant positive slopes. While the slopes of Slot 3 and 4 are negative. Both slopes in positive and both slopes in negative direction show differences in their in- and decreasing. This circumstance declares them suitable to get separated into the needed segments. In turn Slot 5 includes the last 40 seconds instead of 20 seconds, because there are only 5 Slots available and the decrease of the mass concentration is steady (FIGURE 13). These circumstances again accommodate quite well together and generate the completion of the measurement interval for the PST test.

The analysis is man made by human hand and eye. The samples got out of custody and the glass slips examined under a microscope. The custody must of course ensure the further protection of the samples In other words: During the analysis it is the first priority to keep the petri dishes closed. Under the microscope the glass slips get examined and searched through for fibres. These fibres get documented in the labour-diary and photographed for the following measurement.

Because the particles and fibres have to be distinguished, counted and measured by human eye, the needed magnification by the microscopy is an important aspect for the analysis. The needed magnification to see the particles is too big and makes the pictures for the documentation too small. This is why the count of all particles is a process which should be avoided. Thus is the effect of the Brownian motion to distribute (Chapter 3.2) particles evenly used to justify the cut down of the amount of picture down to three **r**epresentative **p**ictures (**RP**). The spherical particles photographed on this RPs (PICTURE 7) become classified and the amounts of the classified spheres get averaged. As a result of the averaging and the Brownian motion it is allowed to declare the outcome statistically representative. The average is only representative for the format of the pictures from the associated slot of the test series. To adapt it to the entire plane of the glass slips or of the Stokes-Chamber the average must be extrapolated.

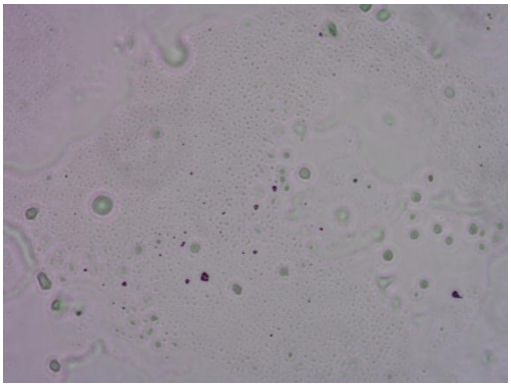

PICTURE 7. Example of representative picture (Aaron Peix 2011)

The linear extrapolation of the particle counts from the microscopy pictures goes through a factorization of the particle amount. The factor is a gradient coming out of the division of the associated surfaces:

$$F_1 = \frac{A_{GS}}{A_{MP}} = \frac{(18*18)*10^{-3}*10^{-3}*\cancel{m^2}}{(550*410)*10^{-6}*10^{-6}*\cancel{m^2}} \quad , \qquad (4\text{-}2)$$

with A_{GS} Area of the glass slips, $A_{GS} = (18\,mm)^2$

A_{MP} Area of the microscopy pictures, $A_{MP} = (550 * 410)\ \mu m^2$,

$$\underline{F_1 = 1436{,}807} \quad . \qquad (4\text{-}3)$$

To cover a glass slip with the dimensions of 18mm x 18mm it would be necessary to make 1436,807 (4-3) pictures within their measures of 410µm in the vertical axis and 550µm in the horizontal. This factor (F_1) is to use to extrapolate the amount of spherical particles in the microscopy pictures. Therefor every RP-amount of the certain slot has to be averaged and the average amount of spheres in their size ranges has to be multiplied with F_1 to compute the representative amount of spherical particles caught on the entire glass slip.

Another factorisation is involved. Considering that the glass slip average will not be representative for the whole diameter plane of the Stokes-Chamber (SC). Hence another factor has to be generated:

$$F_2 = \frac{A_{SC}}{A_{GS}} = \frac{0{,}038025 * \cancel{m^2}}{(18*18)*10^{-3}*10^{-3}*\cancel{m^2}} \quad , \qquad (4\text{-}4)$$

with A_{GS} Area of the glass slips, $A_{GS} = (18\,mm)^2$

A_{SC} Area of the Stokes-Chamber, $A_{SC} = (0{,}195)\ m^2$,

$$\underline{F_2 = 117{,}361} \quad . \qquad (4\text{-}5)$$

F_2 will be used also to extrapolate the fibres quantity, but first it is to continue the extrapolation of the RP-averages up to the SCs cross sectional area. It is now possible with the out of F_1calculated glass slip quantity average to generate a representative amount of spheres for every size range by multiply it with F_2. The quicker way is to calculate a direct factor by a division of the SC crass sectional area A_{SC} through the surface covered by the microscopy images A_{MP} like in equation (4-6), but F_2 is necessary for the fibre analysis.

$$F_3 = \frac{A_{SC}}{A_{MP}} = \frac{0{,}038025 * \cancel{m^2}}{(550*410)*10^{-6}*10^{-6} * \cancel{m^2}} \quad , \qquad (4\text{-}6)$$

$$\underline{F_3 = 168625{,}28} \quad . \qquad (4\text{-}7)$$

(4-6) and (4-7) are proven by (4-8):

$$\underline{F = F_3 = F_1 * F_2 = 168625{,}28} \quad . \qquad (4\text{-}8)$$

The averaging and the factorisation for the extrapolation got apply directly within the analysis and these certain calculations are not presented apart. Tables for this analysis take too much space and are except of some chosen results not displayed here.

Fibres get searched all over the slip, documented by photography and later classified. Their amount is already representative for the glass slip and will only be extrapolated from the slips surface again to their theoretical amount all over the SCs diameter plane. F_2 is used for that by multiplication with the size range specific quantities. Out of that come the results of counted fibres for the exposition.

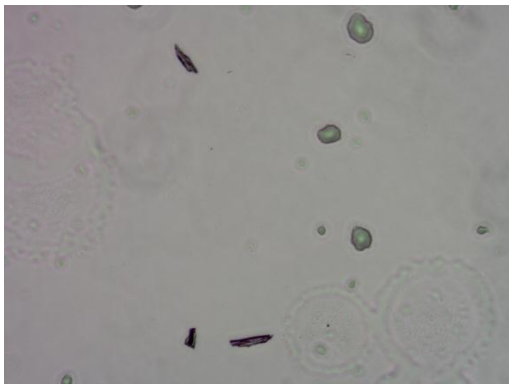

PICTURE 8. Microscopy image; example of fibres in splinter form (Aaron Peix 2011)

Before the procedure of the man-made detection, measurement and analysis will be explained it is necessary to declare the shapes of the searched particles for the distinction. Particles which have at least one dimension twice as long as the other is wide will be identified as fibres. On the pictures are only two dimensions observable. Thus are no more characteristics necessary. All other particles out of this declaration are recognised as spherical particles. The further analysis will nullify mistakes of erroneously identified fibres as the analysis procedure will explain eventual. The definition of the fibre classification covers its different appearances. The most observed are kinds of splinters (PICTURE 8). Because paper is mostly produced out of wood and kaolin it is a near assumption that these splinters are released by the paper. Additionally it is likely that these fibres will not stay in the air for long as they get more distance between them and the source. Hence these splinter fibres got to be produced instantly. PICTURE 9 shows an example of an airborne fibre which can drift through the air carried by *Brownian motion*, drafts and thermodynamics.

PICTURE 9. Microscopy image; example of fibre (Aaron Peix 2011)

For every slot of every used paper series are RPs and photographs of all found fibres done. These images were later examined to find particles and classify them in size ranges related to the BCs categories. The size classifications are: particles smaller and up to 5µm (≤ 5µm); particles bigger than 5µm up to 10µm (≤10µm); particles bigger than 10µm up to 25µm (≤ 25µm); particles bigger than 25µm up to 40µm (≤40 µm); particles bigger than 40µm up to 50µm (≤ 50µm); particles bigger than 50µm up to 100µm (≤ 100µm); particles bigger than 100µm (> 100µm). The over 100µm range is just informational but not included into the comparison because there is no such a size on the BC side. The 6 remaining size categories can now be related to the 6 channels of the BC.

To measure the particles reliable was a ruler template made out of the pictures from a micrometre scale under the microscope. The template is done by tracing the scales horizontal (PICTURE 10) and vertical (PICTURE 11) against the picture them on the screen on a paper. Every digit after the comma stands for 100µm. To warrant the durable accuracy of the measurement of the particles has to happen continuously on the same screen or another fitting template has to be made for the certain used screen. The template is used like a ruler on the screen to measure the particles.

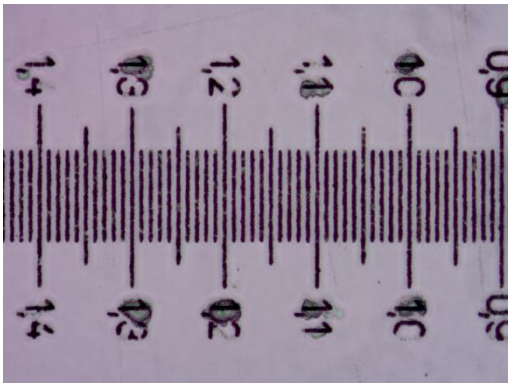

PICTURE 10. Microscopy picture of micrometre scale, horizontal (Aaron Peix 2011)

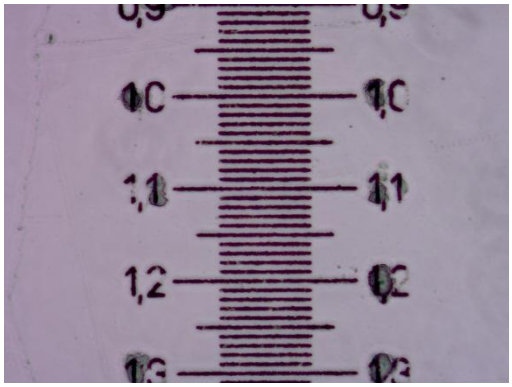

PICTURE 11. Microscopy picture of micrometre scale, vertical (Aaron Peix 2011)

Because fibres can show up in different appearances their classification is to note for both of their dimensions, in width and length. From this point on the PST analysis is split. To gain results exemplary for the slots entirely the fibres results are added to the sphere results after their factorisation. The fibres results of length and width are separately added, to create two different tables which get compared to each other and to the BC results from the prior task. This is an important comparison and should provide the answer to one of the main question of this thesis: How does the BC look on fibres?

The PST test series were prone to errors through the whole man-made sampling. Out of 30 samplings within 10 paper series came only 15 samplings through the procedure without noteworthy troubles. Within these 15 different paper layer tests it was possible to extract only 2 samplings for every layer and none was allowed to came out of the same paper series. The mix out of the paper series variety ensures statistical significance as well as the statistically demanded minimum of 2 samplings for every layer test.

4.2.2 PST-results and comparison with BC

Starting up with the comparison of the cumulative particle counts for 1, 2 and 4 paper layer the focus is first on the different dimensions of a fibre. The fibres got measured in length and diameter. The only to this moment recognised way is to sort the fibres first by dimension, in length and width, and secondly by measures into size sectors. The generated amount of spherical particles is the basis and the amount of fibres in dependence to their length is added and noted in TABLE 8. The amount of fibres in dependence to their diameter is separately added to base-value of spheres and

TABLE 8. Cumulative results of paper layer; PST results, sphere base-value plus fibres separated into their dependence to length and width

	PST		BC
Layers	∑ N (⌀)	∑ N (L)	∑ N of all sizes
1	42749575	42749520	54284
2	115099031	115099209	82283
4	60048455	60047991	139467

noted in TABLE 8 too. Through this process it is possible to nullify any erroneous distinction between spheres and fibres, because of the split addition of the fibres in length and diameter counts results due to a conversion of these fibres into statistical spheres.

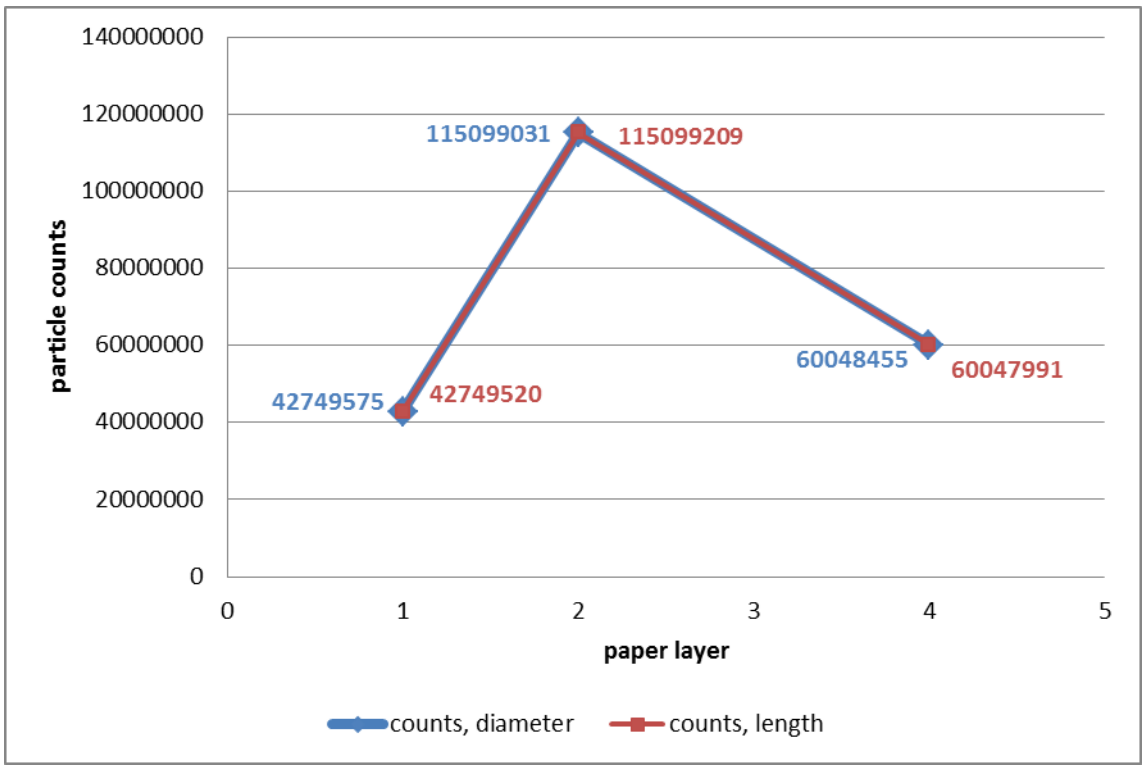

FIGURE 14. PST results, cumulative particle counts for paper layers in dependence of diameter and length

Now it is possible to compare the PST results to each other and to look for the estimated linear behaviour of the growth of the particle counts (FIGURE 14). Different to the BC analysis is here a mathematical standardisation of the values, by converting them into concentration, not possible. The absence of a volume flux bans this option. Hence are the BC counts of 2 minutes sampling also presented in TABLE 8.

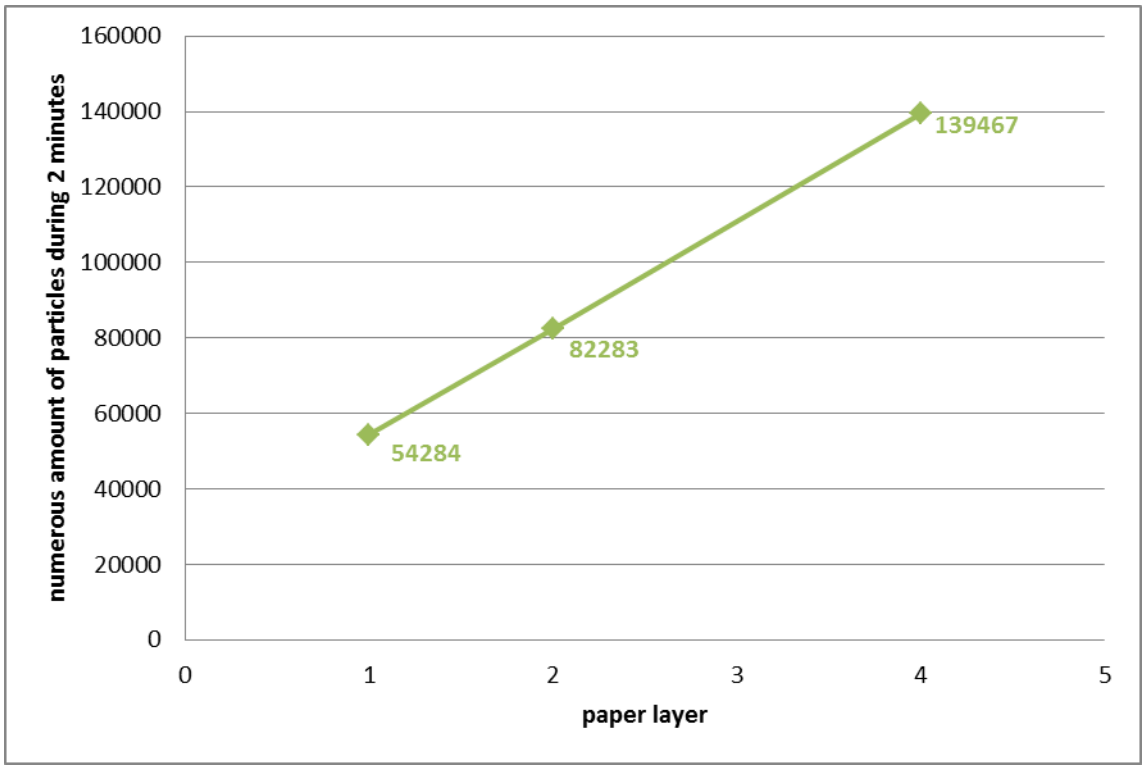

FIGURE 15. BC results, not normalised particle counts per layer over 2 minutes

The PST results differ so strongly from the BC results (TABLE 8) that it is only possible to present them together in a logarithmic scale (FIGURE 16). Both results in a linear scale would display the BC illustration just as a line laying almost directly on the x-axis. Notwithstanding is a solo presentation of the BC counts over the two minutes sampling time recommendable to gain a general confirmation for the use of the not normalised BC results (FIGURE 15). It shows the performance of the particles counts within a linear rise of the paper layers. This is why an accompanied linear count rise is estimated to approve the results validity for the further usage.

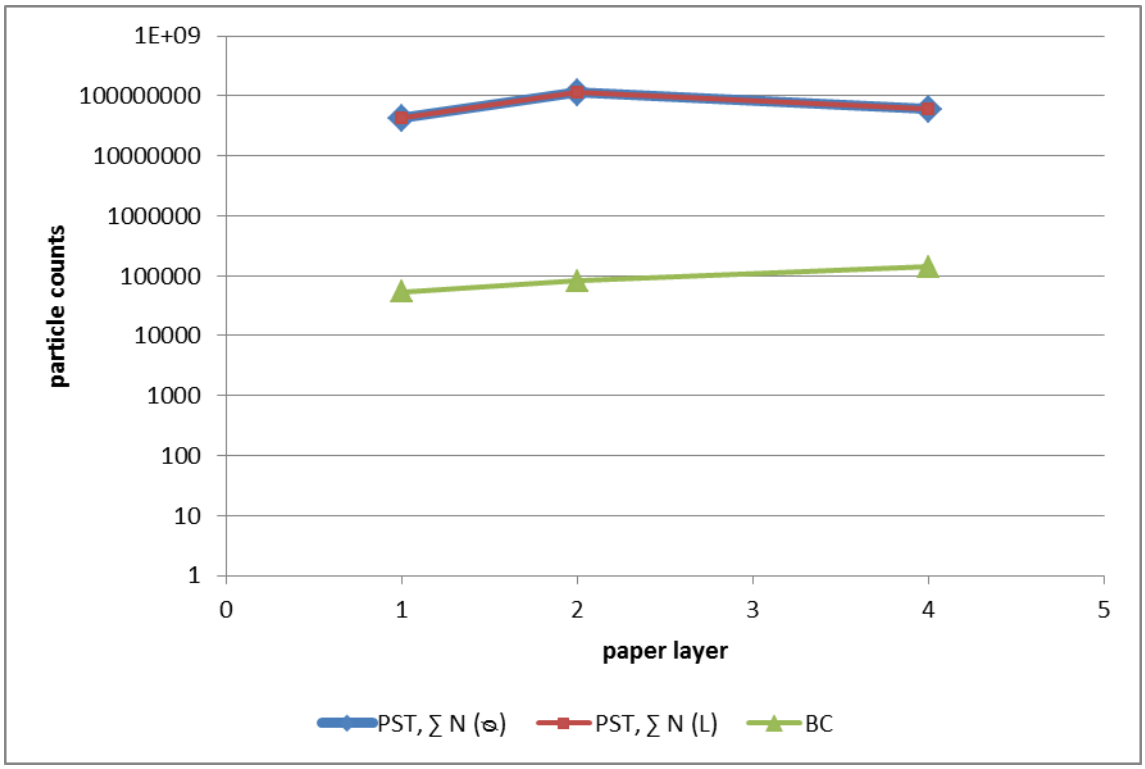

FIGURE 16. BC and PST results, logarithmic scale

A step deeper into the detailed illustration is the presentation and comparison of the PST and BC results in the sampling intervals of the PST (TABLE 2). In TABLE 9 the BC and PST results are listed against each other again. This time are the summed particles of all sizes and layers shown, which are found and eventually extrapolated on their slot/ time segments. To make them comparable it was necessary to generate the exact counterparts out of the BC results. Therefor counts cumulated within the time segments associated to the PST slot switch time interval (TABLE 9).

TABLE 9. BC and PST results, cumulative particle counts of all layers divided into time segments related to the PST sampling interval

BC	Time in seconds		PST	
cumulative sum		Slots	cumulative sum (L)	cumulative sum (ꝏ)
0	0		0	0
32048	0-20	Slot 1	55315207	55315498
126296	20-40	Slot 2	58605981	58605979
65745	40-60	Slot 3	33308434	33308432
26828	60-80	Slot 4	33647561	33647382
12833	80-100	}↓		
12284	100-120			
	80-120	Slot 5	37019538	37019772
12559	(80-120)/2	(Slot 5) / 2	18509769	18509886

It transpired that more adaptations had to be done before it was possible to compare slot 5 with the BC. During the evaluation of FIGURE 4 and the elaboration of the slot interval timetable (TABLE 2) in FIGURE 13, it appeared quite useful to let slot 5 sample over 40 seconds. Afterwards a problem surfaced. In FIGURE 4 it were apparitional that only slide decrease of the particles over the last 40 seconds but when one sums all particles over 40 seconds instead of 20 seconds does the amount just like the seconds double up too. An exact interpolation for the PST result between 80 and 100 seconds is not possible because the value between 100 and 120 seconds is missing also. Thus was the nearest solution to half the amount of slot 5 (red marked in TABLE 9) which comes very close tothe actual amount because of the very slightly decreasing value over the last 40 seconds. For a better comparing of the outcomes to each other it is necessary to calculate appropriate value for the BC. Therefore are the BC values of the 80-100 seconds and 100-120 seconds aggregated and the result halved too (brown marked in TABLE 9). This adjustment applies only for the graphical depiction.

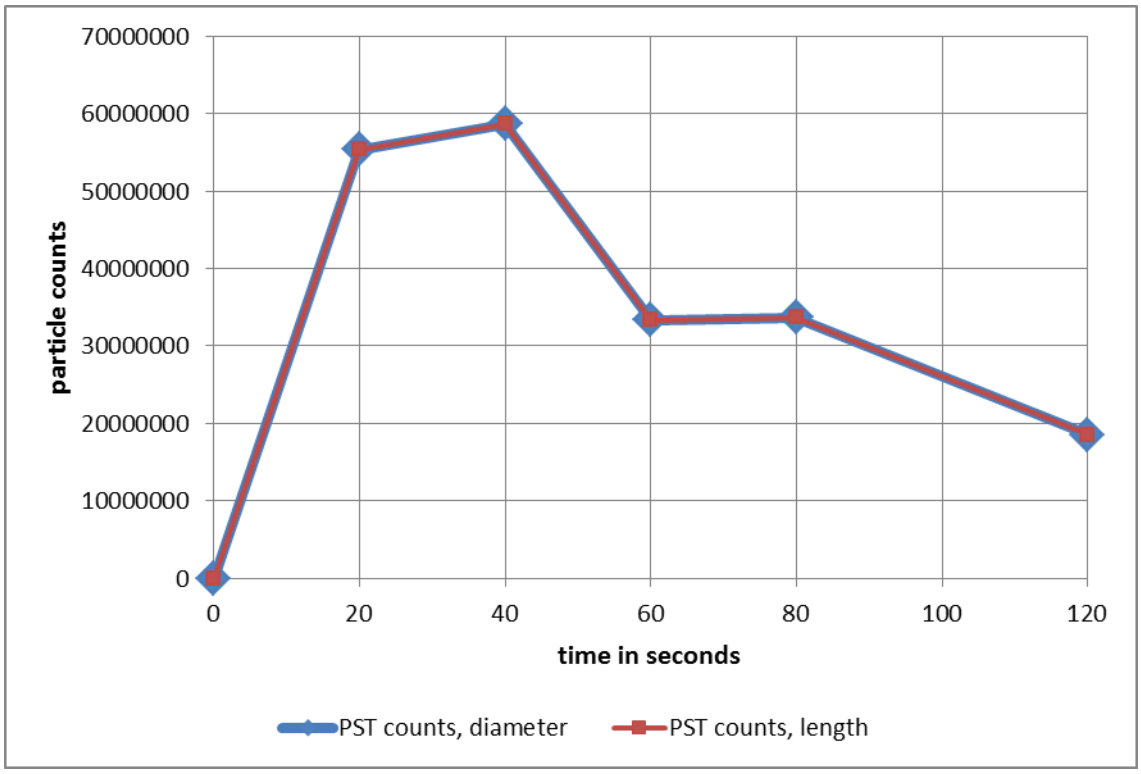

FIGURE 17. PST results, comparison of cumulative particle counts of all layers inclusive fibres in dependence of their diameter and length

Because of the very big discrepancies between the PST and the BC results it is only possible to display them together with a logarithmic scale (TABLE 15). Like in FIGURE 14-16 these results are additionally presented separated too. The PST results for every slot according to TABLE 9 are graphically exposed in FIGURE 17. The in 20 second intervals accumulated BC results are displayed in FIGURE 18.

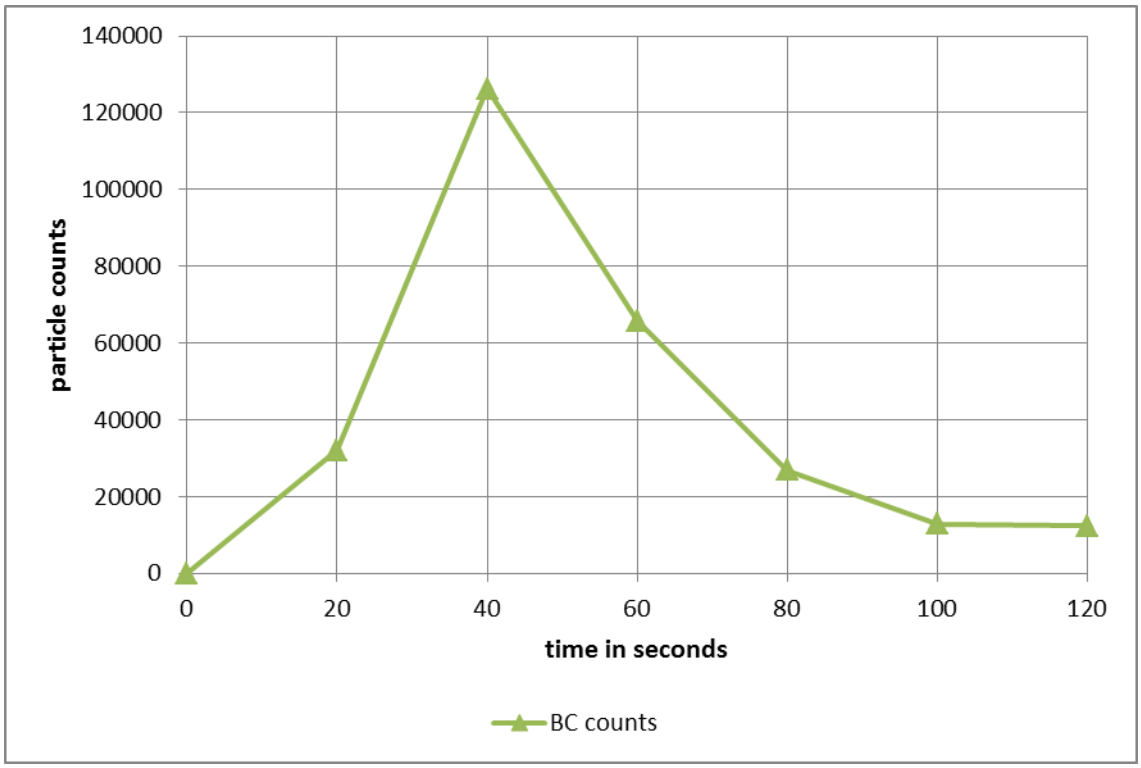

FIGURE 18. BC results, cumulative particle counts of all layers, cumulated in 20 second margins

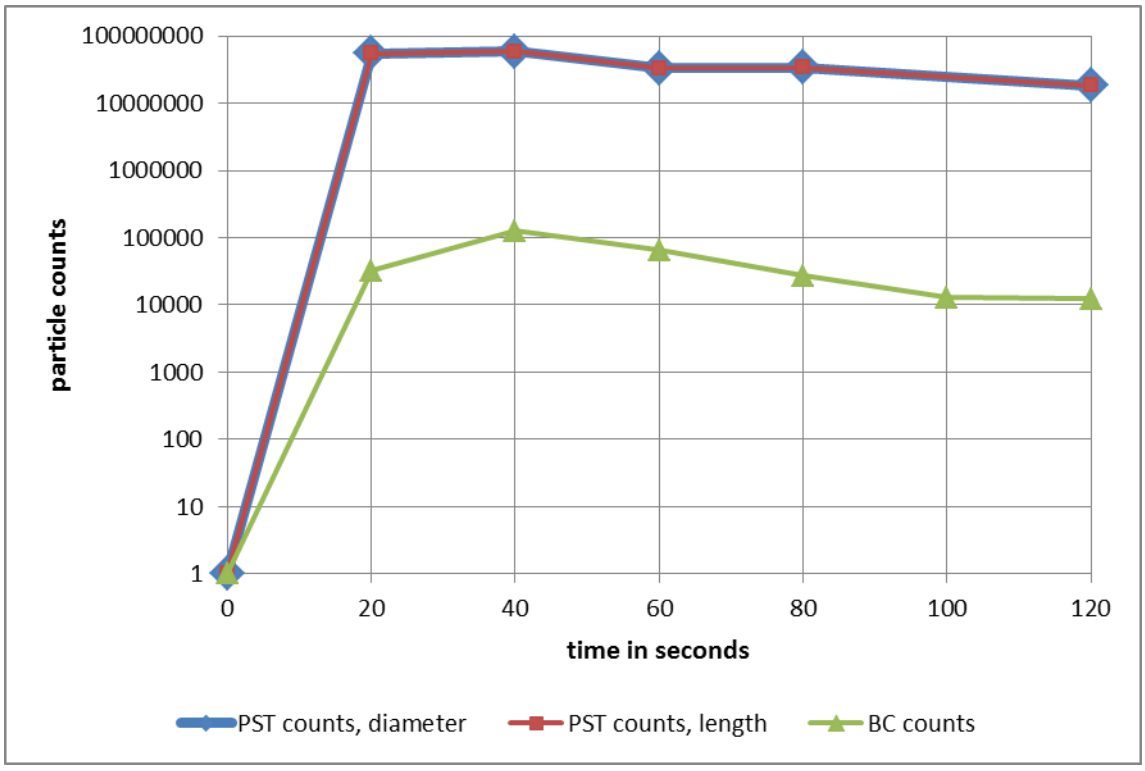

FIGURE 19. BC and PST results, comparison of cumulative particle counts of all layers inclusive fibres in dependence of their diameter and length with BC counts, logarithmic scale

TABLE 10. PST and BC results, divided in paper layers and sampling intervals

	PST						BC			sampling time table
	Average 1 Layer		Average 2 Layer		Single Paper #4; 4 Layer		Average 1 Layer	Average 2 Layer	Average 4 Layer	
	Diameter	Length	Diameter	Length	Diameter	Length				
Slot 1	6577035	6577036	30355722	30355664	18382741	18382507	13846	4723	13479	0-20
Slot 2	10033912	10033913	37605787	37605787	10966280	10966281	22779	39991	63526	20-40
Slot 3	8938082	8938024	15263173	15263114	9107177	9107296	10226	22666	32853	40-60
Slot 4	7082733,5	7082734	11552888	11553183	15011760	15011644	4524	8464	13840	60-80
Slot 5	10117813	10117813	20321462	20321462	6580497	6580263	2909	6439	15769	80-120
Slot 5/2	5058906,3	5058906,5	10160731	10160731	3290248,5	3290131,5	1454,5	3219,5	7884,5	(80-120)/2

The next step of the analysis is even deeper and presents the demeanour of the single layers over the sampling intervals. The results of the paper layers for the BC and the PST tests in sampling interval are listed in TABLE 10. The figures which eventual develop out of it are again equipped with the associated data to facilitate the comparison. FIGURE 20 shows the PST counts of the paper layers which include the sphere count basis and the fibre counts depending on their diameter (TABLE 10). FIGURE 21 actually shows the same exempted from the fibre count input which depends on their length (TABLE 10). The comparison is complete with FIGURE 22 which contains the BC results (TABLE 10).

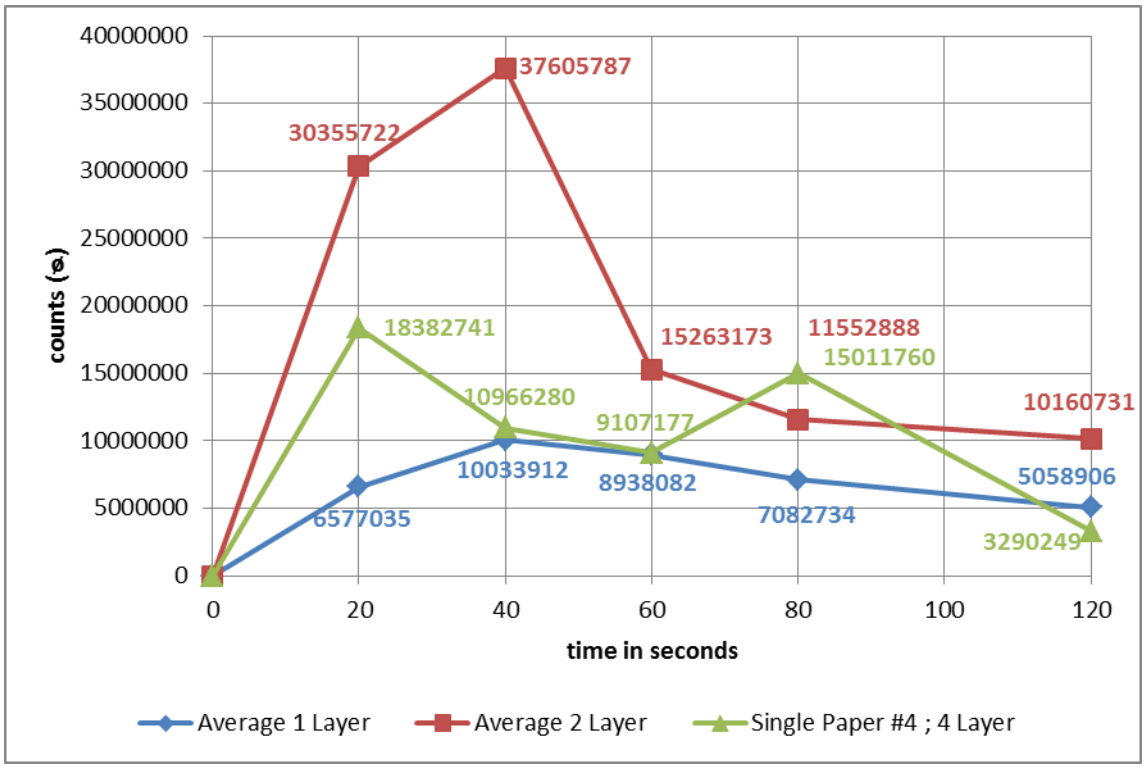

FIGURE 20. PST results, cumulative particle counts within the Slot-intervals depending on their diameter separated into layers

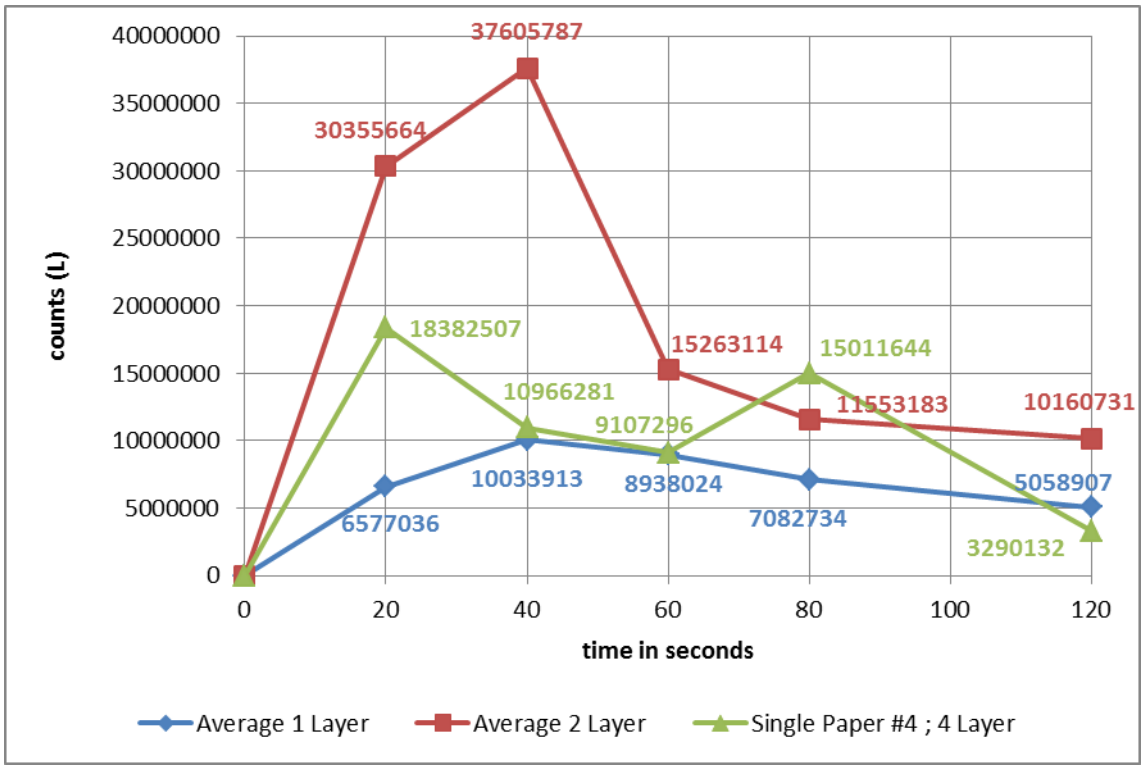

FIGURE 21. PST results, cumulative particle counts within the Slot-intervals depending on their length separated into layers

Unfortunately the basis for the 4 paper layer series analysis is tremendously challengeable. There is only the outcome of a single test series in use during this PST analysis and hence was it impossible to compute an adequate average. The 4 paper layer series was planned to consist out of two 4 paper layer test series: out of the fourth single paper series with the signature 4_4 and out of the fourth double paper series with the signature D4_4. The use of both outcomes was disabled because D4_4 yielded 415 pictures of fibres with several pictures containing multiple counts of fibres. Because paper 4_4 had only 125 images D4_4 was tagged as a statistical outlier and declined to enter the analysis.

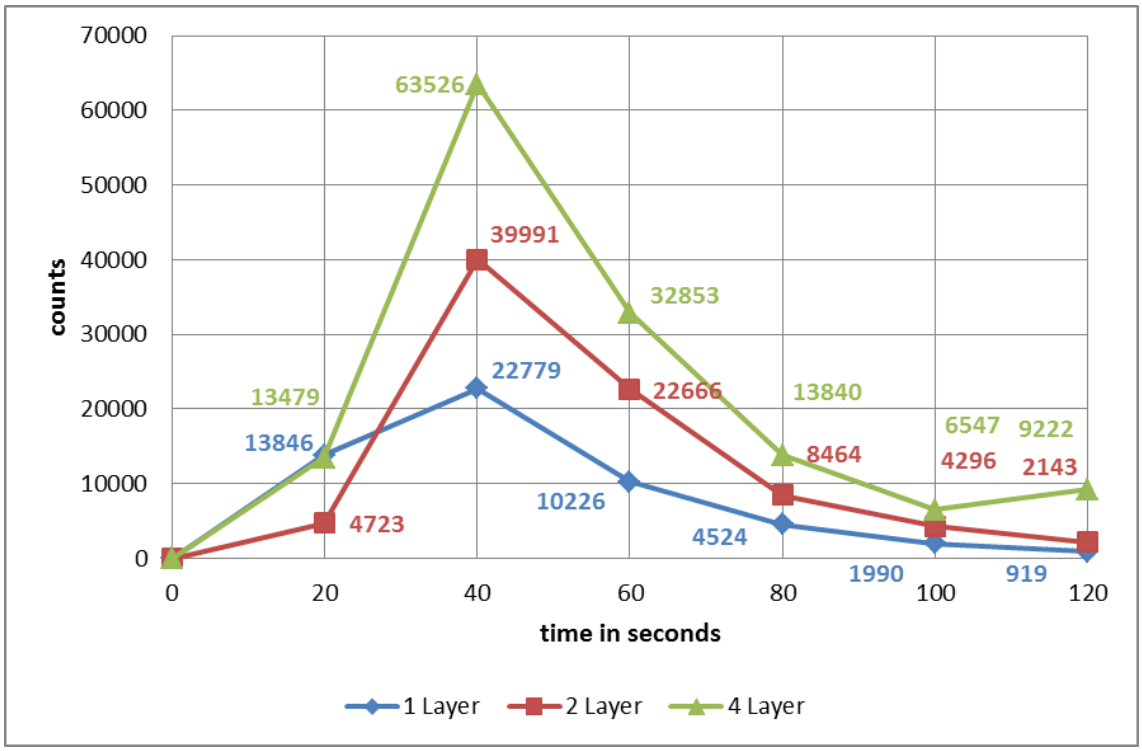

FIGURE 22. BC results, cumulative particle counts within a 20 second interval in accordance to the PST-Slot-intervals separated into layers

4.3 Interferences and Errors

This sub-chapter is designated as a list of negative influences and circumstances which effect directly on the measurement conditions and analysis of the gained data. The following points are of course intended to get applied in the discussion (Chapter 5). The list form shall provide the opportunity to keep an overview of the aspects which oppose to the statistical significance of this investigation.

(a) The result of the Reynolds number calculation (3-36) does not range in the Stokes´ area (TABLE 1). This does not conform with the basically idea of the labour tasks and the purpose of the **S**tokes **C**hamber (**SC**).

(b) No Cleanroom condition during the sampling tasks. Background contamination caused by always present airborne particles influence the PST test series the most. During the preparation of the glass slips for adhering particles, their transportation and analysis opens the possibility of an unwanted contamination after the sampling. Example: Paper D4_4.

(c) A mistake during the manual counting and classification of particles for the PST analysis adds up through the analysis (Chapter 4.2.1).

(d) Selection of the reference pictures (RP) depends on man-made choice. RPs could be wrong done at wrong areas.

(e) Not enough PST test series. Human mistakes ruined the most of the PST samples. Two samples are the minimum for a statistical relevance. Paper D4_4 got declined because of the suspicion of contamination.

(f) Estimation that DT and BC suck all particles from above is unverified.

(g) SC is open on the up and the down side. This could affect the volume flow because the air streams in from up and down side and that anon emerges doubts for the calculation of the air stream velocity through the SC.

(h) DT and BC share the paper ejected particles. They could steal each other the particles if the sampling suction disturbs the evenly distributed particle settlement. That would have an effect on the original gained data intensively.

(i) Movements and temperature changes can create drafts which wind up irritations in the very nearness to the SC. These affect the conditions inside the SC.

(j) No verification that Brownian motion caused equilibrium of particle distribution took place in time before the particles reached the sampling ends of the devices.

(k) Electromagnetic fields and agglomeration could interfere with Brownian motion, but according to Mewis & Wagner can electrostatic effects often be ignored (2012, 36).

(l) Particles which collide with surfaces adhere there (Hinds 1999, 160) and could build aggregates. The accumulation of particles could have caused the PST two-layer incident if they got released from surfaces at once.

5 DISCUSSION

Based on the assumptions, conclusions and the results coming out of this thesis I cannot verify the accuracy of the *Boulder Counter*. Especially the comparison of the BC and PST gave indications that the BC has an upper limitation for the amount of particles it can monitor. In FIGURE 20/21 and 22 the only comparable curve is the one for one paper layer. Not the quantities are the commonalities but the behaviour over time. The immense quantity discrepancies and the observation that the rise of the paper layer is accompanied by the rise of the particle amount are evidence for the limitation of the optical detection technology which bases in general on light scattering and dimming (Chapter 3.2). This effect is explained with the circumstance, that particles which are hidden behind bigger particles cannot get detected. Because the particles in the foreground of the detecting light ray prevent the light to get in contact with particles hidden behind and to measure them. This affects the accuracy enormously.

Almost the same incident can be observed in the comparison of the BC with the DT. FIGURE 10 is a simultaneous increasing and decreasing of the $c(m)$ viewable. The only exception of the similarity is that the DT results are at the peak and stay doubled until the end of the sampling time in which both approach to zero. With the double of the particles released in the two paper layers test series another step happened into incomparability (FIGURE 11). The results peaks are a clear sign for that. Their appearances are separated by 10 seconds and their similar jumps disappear after 30 seconds while it stopped in FIGURE 10 after 37 seconds. In FIGURE 12 the temporal gap between the peaks is grown to almost 20 seconds and no similarity in the manner of the fluctuations is recognisable anymore. While this behaviour actually also opposes the liability of the DT, are the DT results confirmed through its linear rise (FIGURE 7) and its plausibility (FIGURE 4).

The FIGUREs 5 and 6 display the immense varieties between the calculated $c(m)$ of the BC, confirmed by FIGURE 9, and the out putted $c(m)$ of the DT. When displayed together they got no commonalities. Next to quantity the slope of the graphs does also differ from each other. This reminds of the circumstances in FIGURE 9. In FIGURE 9 are the mass concentrations of all size ranges of the BC illustrated. Its outcome is explained with a string of insights: the smaller the size, the bigger the amount, the stronger the slope. The appliance of this perception to FIGURE 6 tallies its outcome and approves the assumption that the BC in general is not able to record all particles which flow through its sensors.

Because of the reasonable linear rise of the BC (FIGURE 8, 9) and DT values (FIGURE 6, 7) a general validity of the devices is proven and makes it difficult to claim any devices broken or not able to perform correctly. Only the huge discrepancies between the qualities lead to the conclusion of an upper limitation of the BC. That is why I can only recommend a usage of the device in very low contaminated ambiences, for example would the monitoring of a cleanroom be a perfect fit for its ability. A usage in industry with enormous emission exceeds the capabilities of the BC.

Another reason for the occurrence of the immense divergences between the BC results and all comparison partners is the possibility of a loss of particles due to the segmentation into the measured size ranges of the BC. If the BC does sort the particles in size ranges like assumed prior (Chapter 3.2) the amount of mis-distributed particles can impossible be that high, that it would explain the lack of detected particles. On the other hand it could be possible that the BC only measures particles in the size of the detectable and outputted sizes. Then there would be a much bigger absence of particles in its results. The latter is unlikely because a technology which detects like that would be very inadequate. A further reason could be the open lower side of the SC. The volume flow could get fed by air from downside which does not include the produced particles. When this could have had an effect on the sampling, than both devices would get the same diluted air considering the equilibration of the stream velocities (Chapter 3.3.2).

The PST findings are quite shaken by their vulnerability. The preparation of glass slips, the finding of the particles, the selection of the RPs, the transport and the custody of the samples, all these factors lift the error percentage and they also got within their task additionally possibilities of failure. It is impossible to overcome all negative influences. After the exclusion of the failure samplings there only was one sample for the four paper layer test left. These inconvenient circumstances are fatal for the PST analysis, at least for the 4 paper layer series. Hence the 4 paper layer analysis is declinable at all. On the other hand the *Brownian motion* is a force that gives a push into the direction of applicability for every single series of measurement. Nevertheless, the PST results of one layer and two layers do still have their statistical significance. In FIGURE 20 and 21 is the situation displayed.

Like FIGURE 7 and 8 for the DT/BC comparison is FIGURE 14 crucial for the general accreditation of the whole analysis. As a matter of fact FIGURE 14 shows a not-linear behaviour. The two layer series has an immense rise of particles which got nothing in common with the 2 layer results of the BC or the DT. In hindsight the SC should have been cleaned after every test series to avoid that too many particles adhere (Hinds 1999, 160) on the inside surface of the SC. This effect could have caused a release of aggregates which got too heavy or more likely got shaken of the surface by tremor. Thence an unrepresentative amount of particles could have been sampled and would shatter the analysis.

Again, the results are not comparable with the BC results due to an enormous difference of the quantities and the behaviour over the time is also, except the peak at second 40, not comparable. The main reason for the incomparability is that the particle counts differ even at the lowest peak of the PST test in ranges of 10 to the power of plus 8 (10^8). These numbers came out of a factorisation which is a linear extrapolation and got granted by the linear behaviour of the BC and DT (FIGURE 7, 8). Additionally FIGURE 17 shows none differences of the values in case of the fibres diameter or length. They are graphically almost identical. These two outcomes make it impossible to come to any conclusion which could lead to an answer to the question if the BC is able to distinguish between fibres and spheres. The lack of detected particles disables also any assumption to multiple counted fibres and prevents any possibility of different comparison.

During the analysis of the PST sampling several particles were found which are excluded from the ranges of the BC. But even those bigger particles would not give enough value - only if counted repeatedly hundred thousand times - and the under 5 µm sized particles do not give enough matter to the analysis. Besides it is impossible to add their counts to any size range because one does not know where to add them. Furthermore does the lack of a volume flow during the PST series avoid the generation of a concentration, for the purpose of a more reliable comparison with the DT.

Several other facts and theoretical ideas compete here to give the deciding reason to declare this assessment as statistical not significant or as significant. Some claim big influences, some nullify each other. Succeeding the noteworthy ascendancies are edited. Notwithstanding are enough data gained to give an adequate assessment for the here recognizable BC possibilities. On the other hand it is impossible to answer the main thesis questions.

A crucial unclearness is the predictability of the *Brownian motion*. The equilibrium of the particle concentration due to the *Brownian motion* is the base of the theoretical idea of this thesis. It is unknown, if the 60 centimetres free fall is enough for the particles to distribute evenly as assumed. This unknowingness coupled with the mathematical fact that are no Stokes´ drag conditions within the SC during the BC/DT tests shake the foundation of this evaluation. Despite the adjustment of the sampling stream velocities which calmed the drag within the SC (Chapter 3.3.2), the combined air flow of the devices is an undeniable fact which got a tremendous effect to the Reynolds number (3-14). Out of this calculations came a theoretical settling time for a spherical particle by the size of 100 µm in (3-45) and (3-48) which did not prevail in any test and proves that there are unpredictable happenings considering diffusion and *Brownian motion*.

Recapitulating the circumstances and the quality of the manual PST sampling series and BC/DT combination I come to the following conclusion: Because of the fact, that the processes got standardised and thus the disturbances for every repeated task got repeated as well, the statistical significance of the BC/DT comparison is sufficient. Hence the cognition of an upper limit for the BCs ability to count and measure particles accurately is appropriated. The comparison of the single paper layer PST analysis with the BC is granted by the fact that during the standardised procedure no failures were documented and no indications of its invalidity were found.

In hindsight should some adjustments applied to the tasks, to improve the validity of the experiment. The devices should sample separately and the results get normalised in concentration afterwards. This should prevent the possibility of an uneven distribution of particles to the devices. Coloured paper should give an immense improvement to the PST sampling. Coloured particles give a good contrast to a perhaps suitable different coloured background for a better distinction of the particles. A cleanroom, adequate clothes and automatized procedure can preserve the experiment and its finding from background contamination, draft influences and thermodynamics. These arrangements will help, but to get comparable results it is necessary to reduce the particle production down to a level in which the BC works accurate.

6 REFERENCES

Arvela, P. Lecturer. 2011. Tampere University of Applied Sciences. Tampere.

Hinds, W.C. 1999. Aerosol Technology. Properties, Behaviour, and Measurement of Airborne Particles. 2nd Edition. New York: Wiley-Interscience.

Lighthouse Worldwide Solutions. 2012. BOULDER COUNTER. 19.07.2012. http://www.golighthouse.com/counter/boulder-counter/.

McPherson, M. The aerodynamics, sources and control of airborne. [PDF]. 21.07.2012. http://www.mvsengineering.com/filelibrary/file_23.pdf.

Mewis, J. & Wagner, J. 2012. Colloidal Suspension Rheology. Cambridge: Cambridge University Press.

Pole, M. How to Select a Particle Counter for my Cleanroom. [PDF]. [Lighthouse Worldwide Solutions]. Read 15.08.2011. http://www.golighthouse.com.tr/media/How_to_Select_a_Particle_Counter_for_my_Cleanroom.pdf.

Schwartz, R. & Lindau, A. 2002. Das europäische Gravitationszonenkonzept nach WELMEC für eichpflichtige Waagen. 18th IMEKO-TC3Conference. 24.-26.09.2002. Celle.

Schweizer, A. 2012. Hydraulischer Durchmesser bei rechteckiger Querschnittsform. Updated 28.04.2012. Read 27.04.2012. http://www.schweizer-fn.de/stroemung/druckverlust/v2_druckverlust.htm#hdurchmesserrechteck.

Seinfeld, J. & Pandis, S.2006. Atmospheric Chemistry And Physics. From Air Pollution to Climate Change. 2nd Edition. Haboken: John Wiley & Sons, Inc.

Stieß, M. 01.04.2005. Einführung in die Verfahrenstechnik: 8 Sedimentation. [PDF]. Read 25.05.2011. http://mb-s1.upb.de/steam-cdtf/Verfahrenstechnik/8%20%20Sedimentation.pdf.

The Engineering ToolBox. STP - Standard Temperature and Pressure & NTP - Normal Temperature and Pressure. Read 30.05.2012. http://www.engineeringtoolbox.com/stp-standard-ntp-normal-air-d_772.html.

7 APPENDIXES

APPENDIX 1: 1 (4)

CALCULATION BASIC VALUES

- Density of air ρ_{Air} :

  Out of the *Ideal Gas Law* (3-15) it is possible to generate the air density under the conditions of the experimental environment which conform to the NTP-conditions:

  $$p * V = m * R_i * T \quad , \qquad (3\text{-}15)$$

  with p Pressure; ambience pressure: $p_{amb} = 101{,}3\ kPa$

  V Volume

  m Mass

  R_i specific gas constant: $R_i = R_S = \frac{R_m}{M}$,

  R_m molar gas constant: $R_m = 8{,}314\ \frac{J}{mol*K}$

  M molecular weight; Air: $M_{air} = 28{,}97\ \frac{g}{mol}$

  T Temperature in Kelvin for 20°Celsius: $T = 293{,}15\text{K}$,

$$\Rightarrow \frac{p_{amb}}{R_S * T} = \frac{m}{V} \quad \| \; \rho = \frac{m}{V} \tag{3-16}$$

$$\frac{p_{amb}}{R_S * T} = \rho \Rightarrow \rho_{air} \tag{3-17}$$

$$\rho_{air} = \frac{101{,}3 * 10^3 \; N * s^2 K *}{m^2 * 286{,}97 \; m^2 * 293{,}15 \; K} \quad \| \; 1\,N = 1 \; \frac{kg * m}{s^2} \tag{3-18}$$

$$\rho_{air} = \frac{101{,}3 * 10^3 kg * \cancel{m} * \cancel{s^2 K} *}{m^2 * \cancel{s^2} * 286{,}97 \; m^2 * 293{,}15 \cancel{K}} \tag{3-19}$$

$$\underline{\rho_{air} = 1{,}204 \; \frac{kg}{m^3}} \quad . \tag{3-20}$$

- <u>Kinematic viscosity of air ν_{air}:</u>

$$\nu_{air} = \frac{\eta_{air}}{\rho_{Air}} \quad , \tag{3-21}$$

with $\eta_{air} = 1{,}81 * 10^5 \; \frac{N * s}{m^2} \quad \| \; 1\,N = 1 \; \frac{kg * m}{s^2}$ (3-22)

$$= 1{,}81 * 10^5 \; \frac{kg * \cancel{m} * \cancel{s}}{\cancel{s^2} * \cancel{m^2}} = 1{,}81 * 10^5 \; \frac{kg}{s * m} \tag{3-23}$$

and $\rho_{air} = 1{,}20 \; \frac{kg}{m^3}$ (3-20)

$$\nu_{air} = \frac{1{,}81 * 10^5 \; \cancel{m^{32}} \; \cancel{kg}}{1{,}20 \quad \cancel{kg} \; \cancel{s \, m}} \tag{3-24}$$

$$\underline{\nu_{air} = 1{,}51 * 10^{-5} \; \frac{m^2}{s}} \quad . \tag{3-25}$$

- Average velocity of the drag $\bar{v}$:

  Over the diameter of a flown through tube occur different velocities. The friction between fluid and the tube borders slows the flowing velocity immense down to theoretically zero. In the middle of the tube flows an unbreaked stream and keeps there the maximum velocity. Because of this circumstance is an average velocity used.

$$\bar{v} = v = \frac{Q}{A} \quad , \qquad (3\text{-}26)$$

with Q Volume flow, $Q = (Q_{BC} + Q_{DT})$,

Q_{BC} Volume flow of Boulder Counter

Q_{DT} Volume flow of DustTrack

A Area of the flowed through diameter plane, $A = L_{SC} * B_{SC}$,

L_{SC} Length of the Stokes-Chamber with 0,195m

B_{SC} Width of the Stokes-Chamber with 0,195m,

$$v = \frac{(Q_{BC} + Q_{DT})}{(L_{SC} * B_{SC})} \qquad (3\text{-}27)$$

$$v = \frac{(27 + 2{,}7)\ l}{(0{,}195 * 0{,}195)\ m^2\ min} \qquad (3\text{-}28)$$

$$v = \frac{29{,}7\ \cancel{l}}{0{,}038025\ \cancel{m^2}\ min} \frac{1\ m^3}{1000\ \cancel{l}} \qquad (3\text{-}29)$$

$$\underline{v = 0{,}781\ \frac{m}{min}} \ \underline{= 46{,}864\ \frac{m}{h}} \ \underline{= 0{,}013\ \frac{m}{s}} \ \underline{= 1{,}302\ \frac{cm}{s}} \quad . \qquad (3\text{-}30)$$

- Diameter of the Stokes-Chamber d :

  Because common formulas are developed for circular diameters and the SC has a square diameter, it is necessary to calculate a representative hydraulic diameter d_H (Schweizer 2012) for further calculations:

$$d_H = \frac{2 * L_{SC} * B_{SC}}{L_{SC} + B_{SC}} \quad , \qquad (3\text{-}31)$$

  with L_{SC} Length of the Stokes-Chamber with 0,195m
  B_{SC} Width of the Stokes-Chamber with 0,195m,

$$d_H = \frac{2 * 0{,}195 * 0{,}195 \ m^{\cancel{2}}}{(0{,}195 + 0{,}195) \ \cancel{m}} \qquad (3\text{-}32)$$

$$d_H = \frac{0{,}07605 \ m}{0{,}39} \qquad (3\text{-}33)$$

$$\underline{d_H = 0{,}195 \ m} = \underline{19{,}5 \ cm} \quad . \qquad (3\text{-}34)$$

APPENDIX 2: 1 (2)

RECALCULATION OF THE SETTLING VELOCITY

The recalculation of the settling velocity v_{TS} (Hinds 1999, 55) for bigger Reynolds numbers ($Re > 1{,}0$) goes through:

$$\boxed{v_{TS} = \left(\frac{4 * \rho_p * d_p * g}{3 * C_D * \rho_g}\right)^{\frac{1}{2}}} \quad , \qquad (3\text{-}49)$$

with d_p diameter of particle

g gravity constant in Finland: $g_{Fi} = g_{Finland} = 9{,}82\ \frac{m}{s^2}$

ρ_p density of particles, $\rho_p = 1000\ \frac{kg}{m^3}$

ρ_g density of the medium gas, Air : $\rho_{air} = 1{,}20\ \frac{kg}{m^3}$

C_D drag coefficient, depending on the Reynolds number Re_d.

The drag coefficient C_D (Hinds 1999, 44) computes out of:

$$C_D = \frac{24}{Re} * (1 + 0{,}15 * Re^{0{,}687}) \quad . \qquad (3\text{-}50)$$

Although has the Reynolds number Re to be calculated, but a bit differently than in (3-14). According to Hinds (1999, 28) the viscosity is more exactly integrated into the formulary:

$$Re_d = \frac{\rho_g * \bar{v} * d}{\eta} \quad , \qquad (3\text{-}51)$$

with ρ_g density of the gas medium air (3-20)

$\bar{v}$ average velocity of the drag (3-30)

d by drag flown through diameter, hydraulic diameter d_H (3-34)

η dynamic viscosity of air for 20°C $\eta_{air} = 1{,}81 * 10^{-5}\ Pa * s$ (Hinds 1999, 24) ,

$$\Rightarrow Re_d = \frac{1{,}2\cancel{kg} * 0{,}013\cancel{m} * 0{,}195\cancel{m} * \cancel{m*s}}{\cancel{m^3} * \cancel{s} * 1{,}81*10^{-5}\cancel{kg}} \quad (3\text{-}52)$$

$$\underline{Re_d = 168{,}07} \quad . \quad (3\text{-}53)$$

This result (3-53) can now be inserted into (3-50) for the drag coefficient:

$$C_D = \frac{24}{168{,}07} * (1 + 0{,}15 * 168{,}07^{0{,}687}) \quad (3\text{-}54)$$

$$\underline{C_D = 0{,}867} \quad . \quad (3\text{-}55)$$

Now, as C_D is gained and all other components for the settle velocity (3-49) are here constant and can be used from the prior calculation (Appendix 1), all parts get put together to determinate the speed of a 100µm dust particle with the density of 1000 g/cm^3:

$$v_{TS,100\mu m} = \left(\frac{4 * 1000\cancel{kg} * 100*10^{-6}m * 9{,}82m * \cancel{m^3}}{3* \cancel{m^3} * 0{,}867 * s^2 * 1{,}2\cancel{kg}}\right)^{\frac{1}{2}} \quad (3\text{-}56)$$

$$v_{TS,100\mu m} = \left(1{,}2588\ \frac{m^2}{s^2}\right)^{\frac{1}{2}} = \sqrt{1{,}2588\ \frac{m^2}{s^2}} \quad (3\text{-}57)$$

$$\underline{\underline{v_{TS,100\mu m} = 1{,}12\ \frac{m}{s} = 112{,}2\ \frac{cm}{s}}} \quad . \quad (3\text{-}58)$$

Again with the Stoke-Chamber height of 60cm and the particle speed (3-58) it is to determinate the theoretical settlement time t_{settle}:

$$t_{settle} = \frac{h_{SC}}{v_{TS}} \quad \left\| v_{TS,100\mu m} = 1{,}12\ \frac{m}{s} \right. , \quad (3\text{-}59)$$

$$t_{settle,100\mu m} = \frac{0{,}6\ \cancel{m}\ s}{1{,}12\ \cancel{m}} \quad (3\text{-}60)$$

$$\underline{\underline{t_{settle,100\mu m} = 0{,}53\ s}} \quad . \quad (3\text{-}61)$$

APPENDIX 3

BACKGROUND VALUES

BC: Background sampling

Instrument Model: BOULDER CNTR
Instrument Serial #: 101133001
Downloaded On: 6/ 20/ 2011 14:55:17
Particle Data: Differential
Data Duration: 6/ 13/ 2011 15:59:43 to 6/ 15/ 2011 15:20:19

	Location (Name)	5.0 micron (Counts)	10.0 micron (Counts)	25.0 micron (Counts)	40.0 micron (Counts)	50.0 micron (Counts)	100.0 micron (Counts)	Sample Time (s)	Sample Volume (L)
Average		10,88	5,05	0,10	0,00	0,02	0,00	1,00	0,47
Rounded up		11	6	1	0	1	1		

DT, Background Average : 0,01 mg /m^3

Appendix 4

BC RESULTS, CONVERTION OF THE COUNTS INTO c(m)

all datas reasoned on the averages !

1 Layer		V(Σparticle i) =	m (particle i) =	m (particle i) =	m (particle i) =	average	c (mass) =
Vmeasure (in Liter)=	56,63	Vpi * Ni	Vpi*Ni*ρ(particle)	Vpi*Ni*ρ(particle)	Vpi*Ni*ρ(particle)	Cumulative mass in the sample	m (particle i) / Vmeasure
Vpi ↓↓↓			[ρ(particle) = 1000 kg/ m^3]				
5 µm	Vp(5µm) =	6,54167E-17	3,25016E-12	0,0000033	0,0033	3,2502	3,250	0,057
10 µm	Vp(10µm) =	5,23333E-16	2,33773E-12	0,0000023	0,0023	2,3377	5,588	0,041
25 µm	Vp(25µm) =	8,17708E-15	9,48542E-13	0,0000009	0,0009	0,9485	6,536	0,017
40 µm	Vp(40µm) =	3,34933E-14	4,35413E-13	0,0000004	0,0004	0,4354	6,972	0,008
50 µm	Vp(50µm) =	6,54167E-14	2,61667E-13	0,0000003	0,0003	0,2617	7,234	0,005
100 µm	Vp(100µm) =	5,23333E-13	0	0,0000000	0,0000	0,0000	7,234	0,000
	in cubicmeters	in m^3	in kg	in g	in mg (= 10^-3 g)	in µg (= 10^-6 g)	in µg (= 10^-6 g)	in µg / Liter
2 Layer		V(Σparticle i) =	m (particle i) =	m (particle i) =	m (particle i) =	average	c (mass) =
Vmeasure (in Liter)=	56,63	Vpi * Ni	Vpi*Ni*ρ(particle)	Vpi*Ni*ρ(particle)	Vpi*Ni*ρ(particle)	Cumulative mass in the sample	m (particle i) / Vmeasure
Vpi ↓↓↓			[ρ(particle) = 1000 kg/ m^3]				
5 µm	Vp(5µm) =	6,54167E-17	5,01223E-12	0,0000050	0,0050	5,0122	5,012	0,089
10 µm	Vp(10µm) =	5,23333E-16	3,19652E-12	0,0000032	0,0032	3,1965	8,209	0,056
25 µm	Vp(25µm) =	8,17708E-15	1,03849E-12	0,0000010	0,0010	1,0385	9,247	0,018
40 µm	Vp(40µm) =	3,34933E-14	4,68907E-13	0,0000005	0,0005	0,4689	9,716	0,008
50 µm	Vp(50µm) =	6,54167E-14	3,27083E-13	0,0000003	0,0003	0,3271	10,043	0,006
100 µm	Vp(100µm) =	5,23333E-13	0	0,0000000	0,0000	0,0000	10,043	0,000
	in cubicmeters	in m^3	in kg	in g	in mg (= 10^-3 g)	in µg (= 10^-6 g)	in µg (= 10^-6 g)	in µg / Liter
4 Layer		V(Σparticle i) =	m (particle i) =	m (particle i) =	m (particle i) =	average	c (mass) =
Vmeasure (in Liter)=	56,63	Vpi * Ni	Vpi*Ni*ρ(particle)	Vpi*Ni*ρ(particle)	Vpi*Ni*ρ(particle)	Cumulative mass in the sample	m (particle i) / Vmeasure
Vpi ↓↓↓			[ρ(particle) = 1000 kg/ m^3]				
5 µm	Vp(5µm) =	6,54167E-17	8,02761E-12	0,0000080	0,0080	8,0276	8,028	0,142
10 µm	Vp(10µm) =	5,23333E-16	5,17524E-12	0,0000052	0,0052	5,1752	13,203	0,091
25 µm	Vp(25µm) =	8,17708E-15	2,0688E-12	0,0000021	0,0021	2,0688	15,272	0,037
40 µm	Vp(40µm) =	3,34933E-14	8,37333E-13	0,0000008	0,0008	0,8373	16,109	0,015
50 µm	Vp(50µm) =	6,54167E-14	2,48583E-12	0,0000025	0,0025	2,4858	18,595	0,044
100 µm	Vp(100µm) =	5,23333E-13	0	0,0000000	0,0000	0,0000	18,595	0,000
	in cubicmeters	in m^3	in kg	in g	in mg (= 10^-3 g)	in µg (= 10^-6 g)	in µg (= 10^-6 g)	in µg / Liter

Appendix 5: 1(2)

MASS CONCENTRATION OF BC AND DT FOR EVERY SECONDS

		DT	BC			DT	BC			DT	BC
	TIME	c (m)	SUM c(m)		TIME	c (m)	SUM c(m)		TIME	c (m)	SUM c(m)
	sec	µg/L	µg/L		sec	µg/L	µg/L		sec	µg/L	µg/L
Average - 1 Layer	0	0,00	0,00000	Average - 2 Layer	0	0,00	0,00000	Average - 4 Layer	0	0,00	0,00000
	1	0,018	0,00883		1	0,01	0,00033		1	0,00	0,00105
	2	0,003	0,01891		2	0,00	0,00118		2	0,00	0,00236
	3	0,005	0,01635		3	0,00	0,00177		3	0,00	0,00242
	4	0,009	0,01465		4	0,00	0,00124		4	0,02	0,00229
	5	0,057	0,02460		5	0,00	0,00105		5	0,04	0,03611
	6	0,131	0,03114		6	0,00	0,00111		6	0,01	0,00307
	7	0,179	0,17898		7	0,01	0,00111		7	0,01	0,00504
	8	0,213	0,19553		8	0,00	0,00203		8	0,00	0,03879
	9	0,140	0,16433		9	0,00	0,00255		9	0,01	0,22209
	10	0,148	0,17604		10	0,00	0,00301		10	0,01	0,06659
	11	0,140	0,12364		11	0,00	0,05763		11	0,05	0,25035
	12	0,163	0,18140		12	0,03	0,05907		12	0,20	0,29771
	13	0,260	0,15510		13	0,03	0,04056		13	0,16	0,36882
	14	0,340	0,26428		14	0,10	0,15137		14	0,19	0,38504
	15	0,417	0,19867		15	0,20	0,17905		15	0,25	0,49762
	16	0,166	0,18853		16	0,13	0,21522		16	0,23	0,48153
	17	0,197	0,20338		17	0,07	0,24132		17	0,24	0,56625
	18	0,198	0,25408		18	0,08	0,14241		18	0,27	0,52961
	19	0,202	0,14725		19	0,07	0,19821		19	0,32	0,52974
	20	0,260	0,25565		20	0,14	0,25244		20	0,23	0,56029
	21	0,269	0,14523		21	0,24	0,30366		21	0,26	0,55349
	22	0,242	0,19520		22	0,21	0,27325		22	0,31	0,55133
	23	0,212	0,14614		23	0,19	0,25140		23	0,46	0,54832
	24	0,230	0,15445		24	0,18	0,31819		24	0,42	0,43633
	25	0,275	0,18585		25	0,25	0,31099		25	0,49	0,44830
	26	0,237	0,19174		26	0,24	0,26147		26	0,54	0,41651
	27	0,229	0,16524		27	0,31	0,28469		27	0,77	0,45118
	28	0,251	0,15249		28	0,26	0,26474		28	0,66	0,40519
	29	0,293	0,18048		29	0,29	0,24250		29	0,68	0,43273
	30	0,336	0,15157		30	0,39	0,27508		30	0,90	0,46217
	31	0,288	0,14182		31	0,50	0,27534		31	0,83	0,41284
	32	0,259	0,13319		32	0,54	0,23184		32	0,85	0,38753
	33	0,246	0,13325		33	0,54	0,23753		33	0,83	0,43692
	34	0,215	0,13751		34	0,58	0,21496		34	0,89	0,40277
	35	0,210	0,13352		35	0,53	0,22778		35	0,92	0,39394
	36	0,217	0,11683		36	0,49	0,23439		36	0,83	0,36162
	37	0,225	0,10434		37	0,41	0,22065		37	0,79	0,36110
	38	0,267	0,10159		38	0,46	0,20986		38	0,78	0,33376
	39	0,221	0,08458		39	0,44	0,19010		39	0,70	0,31622
	40	0,234	0,08740		40	0,40	0,17702		40	0,67	0,27724
	41	0,161	0,08059		41	0,43	0,17610		41	0,61	0,27128
	42	0,153	0,07170		42	0,42	0,16289		42	0,54	0,24198
	43	0,157	0,07000		43	0,35	0,16387		43	0,51	0,24956
	44	0,179	0,06182		44	0,38	0,15975		44	0,46	0,23589
	45	0,174	0,05874		45	0,30	0,14307		45	0,49	0,19861
	46	0,195	0,05626		46	0,25	0,12763		46	0,47	0,18768
	47	0,123	0,05731		47	0,21	0,12796		47	0,42	0,17708
	48	0,103	0,05443		48	0,27	0,11716		48	0,47	0,18748
	49	0,079	0,04815		49	0,24	0,11638		49	0,40	0,17427
	50	0,092	0,04632		50	0,29	0,10362		50	0,30	0,14294
	51	0,105	0,04089		51	0,24	0,09603		51	0,28	0,14058
	52	0,086	0,03958		52	0,24	0,09714		52	0,25	0,13626
	53	0,073	0,04017		53	0,23	0,10172		53	0,29	0,13031
	54	0,077	0,03892		54	0,19	0,08229		54	0,30	0,11958
	55	0,081	0,03637		55	0,26	0,08066		55	0,19	0,11441
	56	0,083	0,03598		56	0,15	0,07150		56	0,16	0,10872
	57	0,128	0,03663		57	0,28	0,06731		57	0,14	0,10055
	58	0,091	0,03264		58	0,17	0,07091		58	0,16	0,12743
	59	0,107	0,03317		59	0,15	0,06411		59	0,16	0,08583

		DT	BC			DT	BC			DT	BC
	TIME	c (m)	SUM c(m)		TIME	c (m)	SUM c(m)		TIME	c (m)	SUM c(m)
	sec	µg/L	µg/L		sec	µg/L	µg/L		sec	µg/L	µg/L
Average - 1 Layer	60	0,073	0,02878	Average - 2 Layer	60	0,16	0,05914	Average - 4 Layer	60	0,15	0,08844
	61	0,089	0,02761		61	0,17	0,05325		61	0,16	0,08478
	62	0,084	0,02780		62	0,14	0,05135		62	0,18	0,07582
	63	0,053	0,02545		63	0,12	0,05031		63	0,21	0,07824
	64	0,086	0,02375		64	0,10	0,04926		64	0,23	0,07889
	65	0,079	0,02466		65	0,14	0,04501		65	0,21	0,07176
	66	0,085	0,02558		66	0,11	0,04291		66	0,22	0,07281
	67	0,066	0,02316		67	0,15	0,04376		67	0,17	0,07608
	68	0,081	0,02375		68	0,15	0,03984		68	0,15	0,06823
	69	0,061	0,02277		69	0,12	0,03729		69	0,12	0,06188
	70	0,056	0,01904		70	0,10	0,03729		70	0,11	0,05645
	71	0,043	0,01910		71	0,12	0,03454		71	0,10	0,05318
	72	0,042	0,01845		72	0,13	0,03395		72	0,10	0,05482
	73	0,067	0,02041		73	0,09	0,03415		73	0,09	0,04959
	74	0,074	0,01936		74	0,09	0,03179		74	0,15	0,08197
	75	0,053	0,01537		75	0,09	0,03147		75	0,09	0,05292
	76	0,059	0,01518		76	0,08	0,02800		76	0,08	0,05488
	77	0,057	0,01492		77	0,07	0,03055		77	0,07	0,05587
	78	0,043	0,01125		78	0,06	0,02859		78	0,14	0,05227
	79	0,033	0,01269		79	0,07	0,02852		79	0,12	0,05135
	80	0,029	0,01007		80	0,08	0,02656		80	0,10	0,04815
	81	0,021	0,01145		81	0,06	0,02787		81	0,14	0,04775
	82	0,028	0,00968		82	0,07	0,02649		82	0,07	0,04278
	83	0,035	0,01079		83	0,05	0,02545		83	0,10	0,03918
	84	0,036	0,01079		84	0,06	0,02375		84	0,04	0,03977
	85	0,039	0,01066		85	0,05	0,02322		85	0,04	0,03546
	86	0,024	0,00890		86	0,05	0,01891		86	0,07	0,03474
	87	0,035	0,00778		87	0,06	0,01976		87	0,09	0,03101
	88	0,024	0,00877		88	0,04	0,01812		88	0,10	0,03094
	89	0,024	0,00818		89	0,06	0,01976		89	0,06	0,02800
	90	0,015	0,00877		90	0,06	0,01956		90	0,07	0,02819
	91	0,032	0,00857		91	0,07	0,01799		91	0,08	0,05920
	92	0,020	0,00621		92	0,09	0,01635		92	0,08	0,02617
	93	0,027	0,00628		93	0,06	0,01596		93	0,07	0,05829
	94	0,022	0,00536		94	0,05	0,01459		94	0,06	0,02427
	95	0,015	0,00602		95	0,07	0,01439		95	0,08	0,02185
	96	0,027	0,00589		96	0,07	0,01361		96	0,10	0,01923
	97	0,008	0,00726		97	0,05	0,01295		97	0,10	0,01799
	98	0,023	0,00576		98	0,05	0,01413		98	0,07	0,01858
	99	0,012	0,00406		99	0,04	0,01433		99	0,09	0,02028
	100	0,011	0,00419		100	0,05	0,01178		100	0,08	0,01936
	101	0,015	0,00438		101	0,04	0,01302		101	0,13	0,01649
	102	0,019	0,00327		102	0,04	0,01106		102	0,09	0,01420
	103	0,022	0,00497		103	0,05	0,01027		103	0,08	0,01393
	104	0,005	0,00347		104	0,05	0,01021		104	0,09	0,01328
	105	0,009	0,00314		105	0,03	0,01001		105	0,09	0,01518
	106	0,010	0,00288		106	0,04	0,00949		106	0,06	0,01197
	107	0,010	0,00327		107	0,05	0,01086		107	0,05	0,01315
	108	0,007	0,00360		108	0,05	0,00955		108	0,05	0,01204
	109	0,016	0,00275		109	0,04	0,00857		109	0,04	0,01217
	110	0,009	0,00334		110	0,03	0,00765		110	0,04	0,00929
	111	0,003	0,00321		111	0,03	0,00903		111	0,03	0,00994
	112	0,017	0,00379		112	0,02	0,00949		112	0,03	0,00870
	113	0,009	0,00393		113	0,03	0,00733		113	0,03	0,00890
	114	0,006	0,00255		114	0,06	0,00837		114	0,03	0,00916
	115	0,004	0,00353		115	0,03	0,00700		115	0,03	0,00778
	116	0,005	0,00301		116	0,03	0,00641		116	0,02	0,00896
	117	0,007	0,00262		117	0,02	0,00563		117	0,03	0,00720
	118	0,009	0,00294		118	0,03	0,00504		118	0,02	0,00778
	119	0,004	0,00242		119	0,03	0,00530		119	0,07	0,00890
	120	0,003	0,00255		120	0,04	0,00432		120	0,01	0,00765